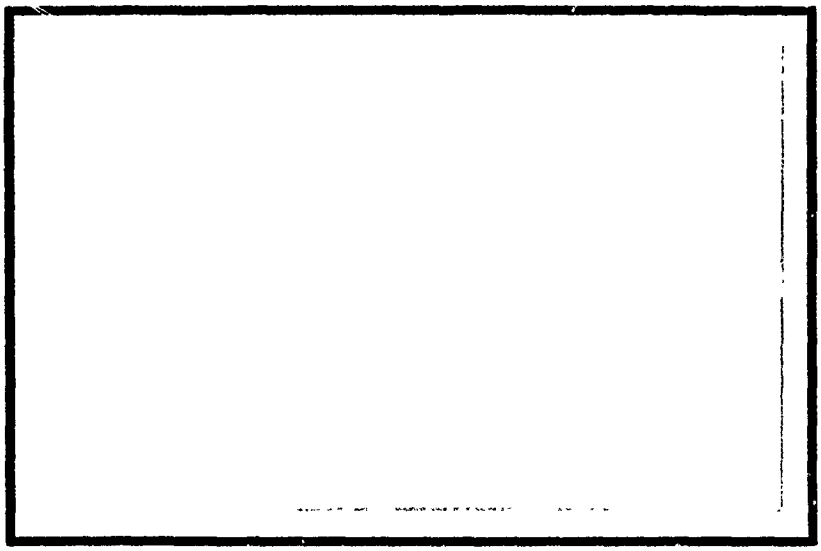

DEPARTMENT OF MECHANICAL ENGINEERING

UNIVERSITY OF UTAH
SALT LAKE CITY, UTAH 84112

Sponsored by Advanced Research Projects Agency
ARPA Order No. 1579, Amend. No. 2
Program Code No. 1F10

UTEC ME 72-027

FRACTURE MECHANICS APPLICATIONS TO ROCK

W. S. Brown
S. R. Swanson
W. E. Mason

FINAL REPORT

Contract No. H0210002

Submitted To
U.S. Bureau of Mines
Twin Cities Mining Research Center
Twin Cities, Minnesota

University of Utah
College of Engineering
Salt Lake City, Utah

February 1972

The views and conclusions contained in this document are those of the authors and should not be interpreted as necessarily representing the official policies, either expressed or implied, of the Advanced Research Projects Agency or the U. S. Government.

Unclassified

Security Classification

DOCUMENT CONTROL DATA - R & D

(Security classification of title, body of abstract and indexing annotation must be entered when the overall report is classified)

1. ORIGINATING ACTIVITY (Corporate author)	2a. REPORT SECURITY CLASSIFICATION
College of Engineering University of Utah Salt Lake City, Utah 84112	Unclassified
	2b. GROUP

3. REPORT TITLE

FRACTURE MECHANICS APPLICATIONS TO ROCK

4. DESCRIPTIVE NOTES (Type of report and inclusive dates)

Final Report 21 December 1970 to 21 December 1971

5. AUTHOR(S) (First name, middle initial, last name)

Wayne S. Brown
Stephen R. Swanson
William E. Mason

6. REPORT DATE	7a. TOTAL NO. OF PAGES	7b. NO. OF REFS
February 1972	92	43

8a. CONTRACT OR GRANT NO	9a. ORIGINATOR'S REPORT NUMBER(S)
H0210002	UTEC ME 72-027
b. PROJECT NO. ARPA Order No. 1579, Amend. No. 2	
c. Program Code No. 1F10	9b. OTHER REPORT NO(S) (Any other numbers that may be assigned this report)
d.	

10. DISTRIBUTION STATEMENT

Unlimited

11. SUPPLEMENTARY NOTES	12. SPONSORING MILITARY ACTIVITY
	ARPA

13. ABSTRACT

Results of a study to investigate the influence of non-uniform stress fields on the failure strength of rocks are presented. Three rock types, Westerly granite, Nugget sandstone, and Tennessee marble, were tested to failure in unconfined tension, torsion, and bending tests, and in triaxial compression and extension tests. Specimens were prepared with notches of various sharpness to vary the intensity of the stress gradients in the specimens. Analyses were performed to determine how the magnitude of the stress varied across the specimen. Two significant experimental observations were made. First, the fracture stress was insensitive to the notch configuration for all rocks tested. Second, local stresses existed in the specimens near the crack tips significantly above the stress required to fracture the rock in a uniform stress field. A preliminary correlation of the increase in strength exhibited by a specimen in a non-uniform stress field is presented based on a critically stressed distance that varies with the maximum stress.

DD FORM 1 NOV 65 1473

Security Classification

ARPA ORDER NUMBER

1579

PROGRAM CODE NUMBER

1F10

NAME OF CONTRACTOR

U. S. Bureau of Mines

EFFECTIVE DATE OF CONTRACT

21 December 1970

CONTRACT EXPIRATION DATE

21 December 1971

AMOUNT OF CONTRACT

$ 55,364.00

CONTRACT NUMBER

H0210002

PRINCIPAL INVESTIGATOR

Wayne S. Brown
(801) 581-7064

PROJECT SCIENTIST

Mr. Syd Peng
(612) 725-4582

SHORT TITLE OF WORK

Fracture Mechanics Applications to Rock

FRACTURE MECHANICS APPLICATIONS TO ROCK

TABLE OF CONTENTS

ABSTRACT

Results of a study to investigate the influence of non-uniform stress fields on the failure strength of rocks are presented. Three rock types, Westerly granite, Nugget sandstone, and Tennessee marble, were tested to failure in unconfined tension, torsion, and bending tests, and in triaxial compression and extension tests. Specimens were prepared with notches of various sharpness to vary the intensity of the stress gradients in the specimens. Analyses were performed to determine how the magnitude of the stress varied across the specimen. Two significant experimental observations were made. First, the fracture stress was insensitive to the notch configuration for all rocks tested. Second, local stresses existed in the specimens near the crack tips significantly above the stress required to fracture the rock in a uniform stress field. A preliminary correlation of the increase in strength exhibited by a specimen in a non-uniform stress field is presented based on a critically stressed distance that varies with the maximum stress.

ACKNOWLEDGMENTS

This research was supported by the Advanced Research Projects Agency of the Department of Defense and was monitored by Bureau of Mines under Contract No. H0210002.

Mr. Lynn Jensen and Mr. Stan Duncan were extremely helpful in conducting the experiments and were assisted by Mr. Jay Rogerson and Mr. Wayd Weber.

FRACTURE MECHANICS APPLICATIONS TO ROCK

I. INTRODUCTION

Most previous laboratory investigations of rock fracture have considered only conditions of uniform stress. It has been suggested that the degree of the non-uniformity of stress may have some bearing on fracture in rock and this has been demonstrated to some extent in rock and other materials. This could be of considerable practical importance as many rock mechanics problems involve non-uniform stresses. A particular example would be in rock cutting where the stress is localized in the vicinity of the cutting tool. Thus, rather than being uniform the stress is highly concentrated. The effect of the non-uniformity of stresses on rock fracture has been recognized by Cook (1) for this problem. Stress gradients occur in other engineering problems where loads are localized or non-uniform.

It appears that improvements in the design of cutting systems will be facilitated by a detailed understanding of the stress and strain fields in the region of rock involved. This approach has been pursued by Cheatham et al (2,3) and Pariseau (4) among others for bit penetration problems. However, this knowledge of the stress field must be accompanied by a corresponding knowledge of the rock fracture properties under the appropriate conditions of high stress gradients.

In the present research program, the objective is to obtain a detailed and quantitative understanding of rock fracture under conditions involving gradients of stress. To accomplish this a series of laboratory tests and theoretical analyses have been carried out. The results and their interpretation are presented in this report.

Previous Work

Although of fundamental importance in many rock mechanics problems, the effects of stress gradients on fracture have been little studied. It has long been appreciated that certain indirect tests for determining the tensile strength of rock, such as bending tests, gave strength values higher than those measured in direct tension. Jaeger and Cook (5) present a discussion of the experimental work on the subject, and present an analysis of the effect

of stress gradients based on critically stressed volume. The size effect on fracture strength has been interpreted by some investigators to be a result of stress gradient effects (6,7). However it appears that little direct work on the effect of stress gradients on fracture in rock has been published.

Stress gradients have been recognized as a variable in materials other than rock. A fundamental theoretical approach is due to Weibull (8) who considered the statistical effect of specimen size on strength. Fracture is considered to result from internal defects, and the statistical defect size and distribution throughout the material introduces a size effect. Stress gradients enter by virtue of the volume of material at a given stress level. A classic result of the Weibull theory is that the strength of a material under uniform stress varies with volume as

$$\frac{\sigma_1 - \sigma_u}{\sigma_2 - \sigma_u} = \left(\frac{V_2}{V_1}\right)^{\frac{1}{m}} \qquad (1)$$

where σ_u and m are material parameters. The details of this have been presented by Jaeger and Cook (5). The use of a Weibull-type statistical theory has been often employed in considerations of brittle fracture. It has been criticized however on the grounds that it is a "weakest-link" type model that is based on catastropic propagation of a crack once fracture has been initiated. It has been established that in many materials considered brittle in some sense, a coalesence of defects is required before final fracture is produced (9). On this basis Hasofer (10) has developed a "parallel-link" statistical model to describe brittle fracture in steel. One of the features of the results is a much less pronounced dependence on size as compared to the Weibull model. The effect of stress gradient on fracture in ceramics has been investigated by Weiss, Chait, and Sessler (11). The apparent stress-strain behavior of their ceramics were linear to the point of fracture and thus would be expected to be sensitive to stress concentrations. The usual maximum stress criteria would predict

$$\sigma_{net} K_t = \sigma_{max} \qquad (2)$$

where K_t is the stress concentration factor. Instead, they found that the ceramics approximately followed the relationship

$$\sigma_{net} \sqrt{K_t} = \sigma_{max} \qquad (3)$$

In this work the weak dependence on stress concentration was explained on the basis of stress gradients by means of the Weibull theory. An alternative interpretation was also suggested that considers a distribution of defects at a given spacing in the material. The ratio of the defect spacing to a length characterizing the stress gradient introduces a size (and stress gradient) effect into the interpretation of fracture. Their model predicts that an inhomogeneous material, as characterized by a large defect spacing, will be insensitive to stress concentrations. This is supported by the findings of Wright and Byrne (12) who introduced various notches into concrete specimens and found a negligible effect on the net section fracture stress in tension.

An experimental study of the effect of stress gradients on stresses in brittle plastics has been presented by Durelli and Parks (13). A strong dependence of fracture on stress gradients was found. Their data were correlated by considering the failure stress to be a linear function of the logarithm of the volume of material stressed above 95% of the tensile strength.

Size and stress gradient effects have been long noted in metal fatigue (14), and are explained by statistical flaw distributions as well as size parameters such as the width of a plastic slip-band. Stress gradients have been considered in spall fracture (15,16); however, this problem is complicated by wavepropagation and strain rate effects.

In the following an experimental program to investigate fracture in Westerly granite, Nugget sandstone, and Tennessee marble will be described. Fracture results will be given for these rocks under a variety of stress conditions, principally involving specimens with stress risers so as to introduce stress gradients. These results will be discussed in detail.

II. EXPERIMENTAL METHODS

Rock Types

Three rock types were tested in this program; these are Westerly granite, Nugget sandstone, and Tennessee marble. All three rock types have been tested previously in this laboratory and elsewhere (17-25).

Specimen Preparation

The tests carried out in this program were tension, extension, and torsion of cylindrical specimens, and bending and compression of prismatic (rectangular) specimens. These tests were carried out on both smooth specimens, and with the exception of the bending tests, on specimens with various types of notches to serve as stress-risers. The notch configurations are shown in Figure 1. The notches can be seen to have tip radii of 1/8, 1/32, and 0.0015 inches.

The cylindrical specimens were cored from large blocks and surface ground on the lateral surface and ends to a uniformity of within $\pm$ 0.0003 inch. The rectangular specimens were cut from the same blocks, and the compression specimens were ground on all sides.

The 1/32 and 1/8 radii notches were produced in the specimens by grinding wheels with semicircular ends. The smallest notch was produced by first establishing a V-shaped notch by grinding, and then further shaping the tip by cutting with a 0.003 inch diameter diamond impregnated wire, thus giving a controlled notch tip radius of 0.0015 inch. The notches formed by these techniques are relatively smooth and reproducible.

The notches for the tension and extension specimens were placed in the circumferential direction as shown in Figure 1. The notches for the torsion specimens were machined both in circumferential and longitudinal directions, as shown in Figures 1 and 2. The smooth (unnotched) extension specimens were 3/4 inch diameter, the notched extension specimens were 1 inch diameter, while both notched and unnotched tension and torsion specimens were 1 inch diameter. All of the notches were placed 1/8 inch deep, so that the net section of the circumferentially notched 1 inch diameter specimens was 3/4 inch in diameter. In addition, tension specimens with a 2 inch diameter were also tested, both unnotched and with 1/8 inch deep circumferential notches. All specimens had an L/D ratio of 2 or more.

In addition to the above specimens, a number of tension tests were carried out on a separate block of Nugget sandstone using a slightly different notch configuration shown in Figure 3. These notches were cut to various depths with a 0.030 thick cut-off saw blade. The notch tips were then sharpened with 0.003 and 0.008 inch diamond impregnated wire. Compression tests were run on the specimen shown in Figure 4. These edge-notched rectangular bars were used for both unconfined and confined compression tests. The specimens used for the bend tests are shown in Figure 5.

In the tests under confining pressure the specimens were jacketed with laboratory Tygon tubing. Since the analysis of the notched specimens under pressure assumes that hydrostatic pressure exists around the surface of the notch as well as on the lateral surface of the specimen, care was taken to ensure that this condition prevailed. This was accomplished by filling the notch with an RTV rubber (Dow-Corning 732) that was soft enough to transmit hydrostatic pressure. Trouble was experienced initially with the Tygon jacket being cut by the sharp edge of the notch flank as pressure compressed the RTV rubber excessively. This was solved by stiffening the notch filler slightly by placing a neoprene rubber O-ring around the notch before filling the remainder of the void with the RTV rubber.

Test Methods

The servo-controlled, electro-hydraulic triaxial testing system used for previous tests (26,27) was employed for both the tension, compression, and extension testing. The apparatus was adapted to tensile testing by constructing the apparatus shown in Figure 6. A proving ring type load cell was designed and fabricated to provide the sensitivity for accurately measuring the small loads encountered in testing brittle materials in tension. Strain gages mounted on the ring provided the stress signal and calibration showed the instrument was both linear and reproducible. The specimen was bonded to metal end tabs using a filled epoxy cement. It was found that this joint was stronger than the rock and no bond failures occurred in these tests.

The extension test apparatus is shown in Figure 7. This test was conducted by applying confining pressure to the specimen with sufficient end load applied to maintain a condition of hydrostatic pressure. The end load was then reduced and since the closure piston diameter is larger than the

specimen diameter the axial stress in the specimen is reduced. This is equivalent to superposing hydrostatic pressure on a tensile test. Some initial difficulty was experienced in the extension test due to fracture of the extension piston. This was solved by using a high toughness maraging steel piston. The axial load in the extension test was measured with a bonded strain gage load cell built into the closure plug and located inside the pressure vessel as shown in Figure 7. Pressure was measured with a manganin coil, and all of the data were recorded on a pen-type Offner recorder.

Alignment of the specimen in both tension and extension testing is a critical problem since bending must be avoided. In both tests the alignment problems were minimized by very carefully grinding the ends of the specimens to ensure parallelism. Universal joints were used in the tension linkage to prevent bending loads being induced by the test machine. The same effect was accomplished in the extension tests by allowing slack in the connecting linkage.

The torsion tests were carried out without confining pressure using a standard laboratory Tinius Olsen torsion testing machine. A special thin-walled steel tube torque cell of appropriate size was designed, constructed, and calibrated for these tests. Strain-gages were used as the output sensors and data were recorded on a Houston Instruments Co. X-Y recorder.

Bending tests were carried out on rectangular specimens 1/2 inch thick by 1 inch wide by approximately 6 1/2 inches long. A four point load apparatus was used as shown in Figure 8. A 10,000 pound Instron Tester was used for these tests.

The compression tests were performed on edge notched rectangular specimens 1/2 inch thick by 1 inch wide by 2 1/2 inches long. These tests were run both unconfined and with confining pressure.

III RESULTS

The results from the tension, extension, torsion, and bending tests are described in this section. The results presented refer in most cases to the average maximum stresses in the specimen, and are based on the minimum cross-sectional area of the notched section for the circumferentially notched

specimens. A consideration of the actual state of stress in the specimens is deferred until the next section. The sign convention employed is that compression is considered positive.

Tension Tests

A summary of the fracture stress for the direct tension tests is given in Table 1. The results are given for both the 1 inch and 2 inch diameter specimens, smooth and with three notch configurations, and for the three rock types. A comparison of the smooth and notched specimen net-section fracture stresses shows that the strength of all three rocks are very insensitive to the presence of the notches. This appears to be a fundamental result, which will be discussed in more detail in the next section. The tension results are seen to exhibit considerably more scatter than compression tests of these rocks. Although this may be an inherent material property, it undoubtedly also reflects the experimental difficulties in direct tension tests. The tensile strength of the Tennessee marble unnotched specimen is in good agreement with values reported by Wawersik (25). Examples of the fracture surfaces are shown in Figure 9.

The results of preliminary tension tests run on Nugget sandstone with a slightly different notch configuration are given in Table 2. These notches were formed by sharpening the end of a 0.030 wide straight notch, as shown in Figure 3. The results are interesting in that several different notch depths were employed. It should be noted that the Nugget sandstone used for these tests was obtained from a different location than that used in all the other studies, and had a somewhat higher tensile strength.

Extension

The fracture stresses for the extension tests (i.e. tension under confining pressure) are given in Table 3. The stresses for unnotched extension specimens of Westerly granite are shown in Figure 10 along with previous results by Mogi (22). It can be seen that the data are in good agreement, although in somewhat different ranges of confining pressure. Similar plots for Nugget sandstone and Tennessee marble are shown in Figures 11 and 12. The net-section stress difference for the notched extension tests is shown in Figures 13-15. The effect of the notches is similar to that seen in the tension tests, and will be analyzed further in the next section. The fractures

in all specimens appeared to be tension fractures, with the surfaces more or less normal to the specimen axis. Typical examples are shown in Figure 16.

Torsion

Unconfined torsion tests were run on unnotched cylindrical specimens, and specimens with either circumferential or longitudinal notches of the configurations shown previously. A summary of the results is given in Table 4. The nominal shear stress which is included has been calculated from the usual formula

$$\tau = \frac{Tc}{J} \qquad (4)$$

where T is the torque, c is the distance from the neutral axis to the outer surface, and J is the polar moment of inertia of the cross section. For the circumferentially notched specimens, the net section diameter has been used. It can be seen that the failure torque is only moderately affected by the notch; thus the nominal shear stress is actually increased. Photographs of typical fractured specimens are shown in Figure 17. The spiral fractures that result from tension fracture can be readily observed in both the smooth and notched specimens.

Beam Bending

Simple rectangular beam specimens were loaded in four point bending. The results are given in Table 5 which shows the failure load, calculated bending moment, and nominal bending stress calculated from the formula

$$\sigma_b = \frac{Mc}{I} \qquad (5)$$

where M is the moment, c is the distance from the neutral axis to the outer surface, and I is the moment of inertia for the cross section. The bending tests were much more reproducible than the direct tension results, and exhibited only nominal scatter. The specimens appeared to break randomly in the central part of the beam. As would be expected, the bending stress is considerably higher than the direct tensile strength for each rock.

Sections were cut in the longitudinal direction from the central part of some of the beams after fracture occurred. These sections were polished and examined with a scanning electron microscope. Typical results are shown in Figures 18-20. Significant defects were observed, primarily associated with grain boundaries. However a comparison of the rock located on the tension and compression sides, and also on the beam neutral axis shows no significant difference.

Notched Compression Tests

Several tests were carried out on rectangular (prismatic) compression specimens with a side notch as shown in Figure 4 . These tests were primarily qualitative and were motivated by an attempt to induce a shear or faulting type fracture, as opposed to the tension fractures characteristic of all the other tests in this program. A typical result is shown in Figure 21 for both unconfined and confined tests. The cracks in the rock specimens appear, however, to be tension cracks. It is not clear at this time if a variation of this specimen configuration may be successful in producing the desired result.

IV. ANALYSIS OF RESULTS

The experimental results presented in the previous section show a complex picture of rock behavior under conditions of stress gradients. In this section the interpretation of these results will be studied.

Fundamental to an understanding of fracture under conditions of stress gradient is a knowledge of the stresses in the test specimens. In general a stress analysis is needed since test specimens with stress gradients are basically statically indeterminate. For specimens with reasonably simple configurations, the stress analysis per se is not an extremely difficult task, particularly as numerical techniques are rather generally available. One of the more successful of these, the finite-element method, was used extensively in this program and will be described subsequently.

The question of the material behavior description to be used in the analysis is more difficult. It is well known that rock is inelastic to some degree depending on the rock type and state of stress, and the authors have previously been involved in the development of constitutive equations (17) for rock inelastic behavior. This inelastic behavior is evidenced even in uniaxial tension. The tension stress-strain curves shown in Figures 22 through 25 illustrate this. These curves, measured by means of strain gaged specimens (18) show two features that are particularly interesting. First, the rock shows bulking (volume expansion) similar to that seen in compression, as evidenced by the lateral strain measurements. Second, hysteresis and permanent set are seen on unloading, particularly in the lateral strain measurements. Similar observations have been made by Wawersik (25). These observations undoubtedly reflect micro-cracking and/or grain boundary sliding.

In spite of these evidences of inelasticity, there is justification for using linear elastic theory in the test specimen stress analysis. First, the non-linearity of the axial stress-strain curves is not large. Even though one may intuitively believe that stresses are considerably relieved by inelastic effects in the immediate vicinity of stress concentrations, this evidence is not readily available as it is not manifested in overall stress-strain curves. Second, even though it may not be possible to calculate realistic stresses in the presence of say, a sharp crack, it has been shown in some cases to be of great utility to use linear elastic solutions. This is the case, for example, in linear elastic fracture mechanics where the use of energy release rate or stress intensity factor can in many cases be based on elastic stress solutions. Finally the relative ease of using linear elastic theory both for the test specimens and in applications is a significant factor. On the basis of these remarks, the specimen stress analysis is being carried out using both linear elastic and nonlinear-inelastic theory. Linear solutions have been carried out and are presented below and used in the analysis of results. The inclusion of inelasticity in the stress analyses is currently under study and will be reported in future work.

Finite Element Analysis

In order to carry out the numerical stress analysis of the cylindrical notched specimens, an axisymmetric finite element computer program was used. This program which was developed specifically for use in this research program, utilizes quadrilateral elements which are made up of four separate triangular elements. Within each triangle the displacements are assumed to vary linearly. Results of analysis of several check cases have shown the program to be very efficient as well as accurate. As previously mentioned, only linear elastic analyses have been carried out for the test specimen configurations to date, however work is currently proceeding on modifications to the finite element program which will allow for nonlinear and inelastic behavior of the rock material.

Finite element analyses have been performed for all six of the cylindrical notched bar configurations. Advantage was taken of the symmetry conditions which allow only one quarter of a bar section to be considered. The finite

element mesh used to represent the one inch diameter bar with a 1/8 inch radius notch is shown in Figure 26. Similar meshes were used to represent the other test specimen geometries with appropriate refinements made in the cases of the notches with smaller radii.

Results of Analysis

The results obtained for the notched cylindrical bars are shown in Figures 27-32. With this information the stress in both the tension and extension test specimens can be determined. This is accomplished by multiplying the stress difference in the test specimens by the appropriate stress ratio from these figures, and then superposing the hydrostatic pressure for the extension specimens. This superposition procedure of course depends on the linearity of the stress analysis. The stress concentration factors obtained from the finite element solutions are presented in Table 6.

As a check on the accuracy of the results a comparison was made with the classic Neuber solution (29). This solution is for a similar configuration with the exception that the notch is assumed to be hyperbolic and "deep" so that the section away from the notch is of infinite diameter. Thus the Neuber solution is appropriate for the specimens only in the immediate vicinity of the notch tip. However, if errors were to exist in the finite element results, they undoubtedly would occur where the stress gradient is highest, i.e., in the vicinity of the notch. A comparison of the results for the one inch diameter bars is given in Figures 27-29. These results show the finite element and Neuber solutions to be in very good agreement near the tips of the notches. Thus, confidence can be placed in the numerical results.

Fracture Stresses in Test Specimens

An apparent result given in the previous section is that the notched rock specimen net section fracture stresses were relatively insensitive to the presence of the notches. On the other hand, this means that the maximum stress predicted at the notch tip is sensitive to the stress concentration factor or perhaps the stress gradient. This can clearly be seen in Figure 33 where the notch tip stresses are plotted vs. the stress concentration factor. A similar effect can be seen in the bending tests, as the maximum tensile stress in the bending specimens is on the order of 60 to 100 % higher than in direct tension.

The differences between the three rocks can be seen more clearly in Figures 34-36 where the net section stress is plotted vs. the stress concentration factor on log-log coordinates. The data have been fitted with a least squares straight line; the slopes of the lines for the three rocks are apparently different.

Critically Stressed Region

One of the methods used in the literature to understand fracture under conditions of stress gradient is to postulate that fracture cannot propagate until the stress reaches a critical value over a finite-sized region. The region may be a critical volume or perhaps a critical linear distance. The size of the region may depend on the distribution and magnitude of the stress in the region. This latter problem is often approached by means of Weibull statistics (8,30), involving the distribution of flaws in the material. As discussed in the introduction, the use of Weibull statistics has often been criticized on the basis that it postulates a "weak-link in series" fracture mechanism, while for certain materials there is a somewhat separate process of the initiation of micro-cracks and the final catastrophic propagation. This has also been approached statistically as well as with more strictly physical concepts such as stress over dislocation-related lengths. In view of the evidences of micro-cracking in rock specimens prior to final fracture for both tension and compression conditions, it seems plausible to investigate the concept of a critically stressed length. This will be approached first by considering only the maximum tension stress in the unconfined tension and bending tests. Subsequently, considerations of the triaxial stress fields will be made.

Tentatively the critically stressed region will be defined by two parameters; the size of the region in which the tensile stress exceeds the direct tensile strength of the rock, and the maximum stress in the region. These two parameters have been plotted, one vs. the other, in Figures 37-39 on log-log coordinates. Included in these plots are the notched 1 and 2 inch diameter specimen tension results and the bending test results. The plots in Figures 37, 78 , and 39 are apparently quite scattered and the implications are not fully evident. To consider this further, it is useful to consider what the limit could be as the stress concentrations are increased. This will be discussed in the following.

Sharp Crack Fracture Mechanics

As the radius of curvature of the notch tip is decreased, the stress distribution approaches that for a sharp crack. In this case the stress distribution is well known (31) and the axial stress on the notch mid-plane in the immediate vicinity of the notch can be written simply as

$$\sigma_{zz} = \frac{K_1}{\sqrt{2\pi r}} \qquad (6)$$

where r is the distance from the crack (notch) tip and K_1 is a constant that depends on the load and geometry and is termed the stress intensity factor. As explained in texts on linear elastic fracture mechanics (9) the value of K_1 at the instant when the crack propagates is regarded as a material property, and if the material is under conditions of plane strain is termed K_{1c}, the critical stress intensity factor for the material. The stress intensity factor K_1 is related to the geometry and loads by a stress analysis, either analytical or numerical (32,33). For example, the stress intensity factor for a sharp crack of length 2c in an infinite plate is given by (32).

$$K_1 = \sigma_o \sqrt{\pi c} \qquad (7)$$

where σ_o is the applied stress at the plate boundary (away from the crack).

The stress analysis for a circumferentially cracked cylinder is available (34) and has been also compared to numerical solutions performed by the author (33). The analytical solution takes the form

$$K_1 = \sigma_{net} f\left(\frac{d}{D}\right)\sqrt{\pi D} \qquad (8)$$

where σ_{net} is the net section axial stress, d is the specimen diameter at the net section, D is the outside specimen diameter, and $f\left(\frac{d}{D}\right)$ is a numerical factor. Thus K_{1c} can be easily calculated from tests of cracked cylinders pulled in tension.

The 0.0015 notch tip radius specimens were designed to simulate sharp crack conditions; this represented the sharpest tip that could be reproducibly

produced using the methods described earlier. Whether or not this tip radius is sufficiently small is open to question and should be investigated further. Taking the position that further sharpening of the notch tip would not affect the apparent strength, K_{1c} values can be calculated from the previous equation. These are shown in Table 7.

The K_{1c} values can be related to the fracture energy for the material by the use of the well known Irwin formula (35)

$$(1 - \nu^2) \frac{(K_{1c})}{E} = G_c = 2\gamma_F \qquad (9)$$

where γ_F is the fracture energy, which includes but is usually much larger than the surface energy specified in the original Griffith fracture criterion. Using the average K_{1c} values, γ_F has been calculated and is shown in Table 8. Also shown are values presented in the literature (25,36-40). The comparison with the previous value of γ_F obtained for Tennessee marble by Wawersik (25) is very close, thus lending some confidence in these results. It should be cautioned that although the present values look reasonable, the extremely close agreement is probably fortuitous.

It is interesting to examine the tests on Nugget sandstone (termed Nugget sandstone II) presented in Table 2 in terms of K_{1c} factors. This sandstone came from a different block than that used in the rest of the program, and had slightly higher tensile properties although apparently the same compressive strength. A number of tests of notched specimens were run on three different notch configurations and four different notch depths. Although somewhat scattered, the results appear to be insensitive to the notch tip radius. Also, if K_{1c} were a material constant independent of notch size, the net section stress for specimens with different notch depths would follow the prediction of equation 8. A comparison of the net section stress in the specimens with that predicted on the basis of equation 8 and an average value of K_{1c} equal to 280 psi $\sqrt{in}$ is shown in Figure 40. Although again the scatter is large, the results could be interpreted to be following the predicted variation.

The concepts of K_{1c} and fracture energy discussed above interact with the concept of a critically stressed distance in the following way. Consider the critically stressed distance vs. maximum stress plots shown previously in Figures 37-39. As the maximum stress is raised, the distance δ over which the stress must be raised above the tensile strength decreases. This distance does not approach zero as the stress gets very large, however, but instead approaches a minimum limit. This can be seen by considering a sharp crack stressed just below the critical stress. As can be seen from equation 6 , the predicted stress is infinite at the crack tip, however, the region δ can be obtained from the stress distribution around the crack. As a first approximation this distance can be obtained from equation 6 by considering r to be equal to δ when the stress is equal to the tensile strength. Thus

$$\delta_{min} = \frac{1}{2\pi}\left(\frac{K_{1c}}{\sigma_{TS}}\right)^2 \qquad (10)$$

and this establishes a minimum value for δ. This expression is approximate as equation 6 only holds for small r. It is interesting to note that a similar expression is commonly used in fracture mechanics for estimating yield zone size, with σ_{TS} replaced by the yield strength (9). These minimum values of δ have been added to Figures 37-39.

Multiaxial Stress Effects

It is possible to generalize the concept of a critically stressed region discussed above to include multiaxial stress effects. To do this it is necessary to consider a function of the full stress tensor as defining the boundary of the critically stressed region, instead of merely the maximum principal stress. A number of possibilities exist for defining this function of the stresses, such as the classical Coloumb-Mohr criteria and others discussed by Jaeger and Cook (5). Other possibilities exist, as for example those discussed by Mogi (28) and Wawersik (2). Rather arbitrarily a uniform stress criterion was selected that is based on the octahedral shear stress and octahedral normal stress. To establish the specific form of the criterion to be used, the fracture values in the unnotched tension and extension tests were employed. The plots could be fitted with a straight line as

$$\text{Westerly granite:} \quad F = \sqrt{J_{2'}} - 0.310\, J_1 - 1.75 \text{ ksi} \tag{11}$$

$$\text{Nugget sandstone:} \quad F = \sqrt{J_{2'}} - 0.346\, J_1 - 0.80 \text{ ksi} \tag{12}$$

$$\text{Tennessee marble:} \quad F = \sqrt{J_{2'}} - 0.33\, J_1 - 1.05 \text{ ksi} \tag{13}$$

where fracture is assumed to take place when F=0. The stress invariants are related to the octahedral stresses and are given by

$$J_{2'} = 1/2\, S_{ij}\, S_{ij} \tag{14}$$

$$J_1 = \sigma_{kk} \tag{15}$$

where S_{ij} is the deviatoric stress and the summation convention is employed. It has been established (21,28) that the above criteria will not predict failure in both triaxial compression and extension experiments. In the present case however only extension type fractures are involved and thus the above limitation may not be serious.

A material distance δ was then defined for each specimen tested with nonuniform stresses, including the notched tension and extension one inch diameter specimens, the unnotched torsion, and the bending test specimens. The distance δ was defined as the radial distance in the cylindrical specimens over which the stresses at the midplane at fracture exceeded the value F=0 that defines fracture for conditions of uniform stress. Similarly δ

was defined in the direction of the beam thickness. Thus the width of the beams and the circumference of the cylinders was ignored.

A variation in δ was observed similar to that seen previously for uniaxial stress. In an attempt to correlate this variation, the values of δ were plotted versus the peak value of F at the notch tip or specimen outer surface. These plots are shown in log-log coordinates in Figures 41-43. Although the plots exhibit a great deal of scatter, general trends can be observed.

The plots of Figures 41-43 are in general quite sensitive to the experimentally determined net section stresses. Changes on the order of 25% or less in the experimental values would make all the points fall in on a straight line, with the exception of the unconfined tension and torsion data. This may well stem from the original choice of the uniform stress criterion for F. Further work on fracture in mixed biaxial tension--compression is needed to answer this question. Systematic difference may be present in the data, as the tension and torsion results are somewhat different.

It should be pointed out that Figures 41-43, although scattered, encompass an extremely wide range of experimental variables. The stresses range from triaxial tension to compression, and exceed the allowable stress for uniform stress conditions by large factors in some cases. Thus, it is significant that the empirical criterion illustrated in Figures 41-43 can successfully correlate the fracture strength.

V. DISCUSSION

One of the fundamental results observed in the experimental data is the insensitivity of net section fracture stress to stress concentrations. This insensitivity has been observed in other materials such as concrete (12), cast iron (14), ceramics (11), and to a lesser extent in plastics (13, 39), steel and aluminum (41). It is widely believed to be due to micro-structural defects and inhomogeneity. As a result of this insensitivity of fracture to stress concentration, linear elastic theory predicts stresses in test specimens under conditions of stress gradient that are greatly in excess of

the fracture stress under uniform stress conditions. Undoubtedly part of this effect is due to the assumption of linear elasticity in the stress calculation, and this assumption will be investigated in future work. However, unlike compression results, tension stress-strain curves of rocks and many of the other materials mentioned above are not greatly nonlinear. Thus, macroscopically observable stress-strain behavior will not furnish a full explanation of the high predicted stresses under nonuniform stress conditions. This observation of increased allowable stress under conditions of non-uniform stress is commonly observed, as for example in the familiar result that the bending strength of brittle materials is higher than the direct tensile strength.

This increase of apparent allowable strength under conditions of non-uniform stress has practical implications. For example, rock cutting inevitably involves concentrated loading. According to the test results described earlier, a rational design of a cutting tool based on rock fracture strength must be based on both the magnitude of the stress and the distance, or perhaps volume, of the stressed area.

A preliminary correlation of the experimental data has been suggested in this report through the concept of a critically stressed distance that varies as a function of the maximum stress. An extremely large range of variables and test conditions has been brought together through this relationship. The plots of this relationship shown in Figures 41-43 are seen to be quite scattered: however changes in the experimental data on the order of 25%, or about 50% for the torsion data, would establish a smooth relationship. Thus, a useful, if ad hoc, relationship seems to have been achieved. Systematic differences in the test results may exist however, and it is hoped that future work may provide a more fundamental explanation of non-uniform stress fracture.

A possible method of connecting "sharp crack" fracture mechanics theory to fracture under conditions of lower stress gradient has been suggested through the critically stressed distance approach. The critically stressed region was seen to decrease with increasing stress gradient, but is postulated to reach a minimum that could be approximated by

$$\delta_{min} = \frac{1}{2\pi} \left(\frac{K_{1c}}{\sigma_{Ts}}\right) \qquad (10)$$

The stress intensity factors (K_{1c}) could be obtained by testing cracked specimens. Values were calculated based on the assumption that the 0.0015 radius notched specimens could be treated as sharply cracked, and good agreement was reached with fracture energy values available in the literature, particularly with the data of Wawersik (25). However, the possibility exists that a sharper notch tip may give different values.

Weiss et al (11, 41-43) have studied the effect of material inhomogeneities on fracture, and have observed in other materials some of the features noted here for rocks. They have developed a rather simple model based on a uniform distribution of flaws as illustrated in Figure 44. Simplifying assumptions lead to an equation for fracture of notched specimens as

$$\sigma_{net} = \frac{\sigma_{Ts}}{K_t} \sqrt{\frac{r + 4x}{r}} \tag{16}$$

where K_t is the exterior notch stress concentration factor, r is the notch radius and x is the distance from the notch tip to the internal flaw. If the flaw spacing is b, an average value of x is b/2 which gives

$$\sigma_{net} = \frac{\sigma_{Ts}}{K_t} \sqrt{1 + 2\frac{b}{r}} \tag{17}$$

which immediately shows that for b=0 (homogeneous material) the notch has its full effect so that

$$\sigma_{net} = \frac{\sigma_{Ts}}{K_t} \tag{18}$$

while for finite b/r (inhomogeneous material) a lower notch effect is seen. It seems likely that a refinement of this approach may furnish an explanation for the experimental data.

Both critically stressed distances and critically stressed volumes have been employed in the literature in stress-gradient fracture, as well as total stressed volume as in the Weibull theory. The difference between these approaches is subtle and it is difficult to justify a choice strictly on the basis of the present data. The critical distance concept has been often employed in metal fatigue, primarily on the basis that a stressed distance is associated with crack growth. On the other hand, the Weibull approach is based on a "weak link in series" concept, and thus may appear

to be more suitable for brittle materials. However, apparent evidence of microcr ck growth in tension well before final rupture were reported here and elsewhere. This clearly is an area for future work.

VI. SUMMARY AND CONCLUSIONS

A test program has been carried out on fracture under conditions of stress gradient on Westerly granite, Nugget sandstone, and Tennessee marble. A wide variety of laboratory test methods were used including tension, extension, torsion, beam bending, and compression. Stress gradients were introduced into the tension and extension test specimens by means of notches. The results were analyzed by means of finite element solutions.

The notched specimen net section fracture stress was found to be insensitive to the notch configuration for all rocks. However, the local stresses in the specimens were much higher than that required to cause fracture in uniformly stressed specimens. This result is typical of many materials, and is evidenced by bending strengths being higher than direct tensile strength in many brittle materials. This apparent increase in strength is undoubtedly important in rock mechanics problems involving stress gradients.

A preliminary correlation of the increase in strength exhibited by a specimen in a non-uniform stress field is presented based on a critically stressed distance that varies as a function of the maximum stress was presented. Although the data were scattered, and systematic differences may also exist, this concept correlates a very large range of variables with reasonable accuracy. The minimum critically stressed distance was approximated by the use of fracture mechanics concepts. This correlation is presented as a preliminary result and will be refined as a part of a research effort currently in progress.

REFERENCES

1. Cook, N. G. W., "Analysis of Hard-Rock Cuttability for Machines," Rapid Excavation - Problems and Progress, The American Institute of Mining, Metallurgical, and Petroleum Engineers, Inc., New York (1970).

2. Cheatham, J. B., and Gnirk, P. F., "The Mechanics of Rock Fracture Associated with Drilling and Depth," Proc. Eight Sym. Rock Mech.: Failure and Breakage of Rock, Port City Press, INc., Baltimore, 410-429 (1967).

3. Cheatham, J. B., Paslay, P. R., and Fulcher, C. W. G., "Analysis of the Plastic Flow of Rock Under a Lubricated Punch," J. Appl. Mech., 35, 87-94 (1968).

4. Pariseau, W. G., "Wedge Indentation of Anisotropic Geologic Media," Proc. Twelfth Sym. Rock Mech., 529-546 (1970).

5. Jaeger, J. C., and Cook, N. G. W., Fundamentals of Rock Mechanics, Methuen and Co. Ltd., London (1969).

6. Brown, E. T., "Strength-size Effects in Rock Material," Mineral Resources Research Center, Prog. Report 24, University of Minnesota, 138-150 (1971).

7. Hodgson, K., and Cook. N. G. W., "The Effects of Size and Stress Gradient on the Strength of Rock," Proc. Second Cong. Int. Soc. Rock Mech., 2, 3-5 (1967).

8. Weibull, W., "A Statistical Theory of the Strength of Materials," Ingeniors Vetenskaps Akademien, Handlingar, No. 151 (1939).

9. Tetelman, A. S., and McEvily, A. J. Jr., Fracture of Structural Materials, John Wiley and Sons, Inc., New York (1967).

10. Hasofer, A. M., "A Statistical Theory of Brittle Fracture of Steel," The International Journal of Fracture Mechanics, 4, No. 4, 439-451 (1968).

11. Weiss, V., Chait, R., and Sessler, J. G., "Fracture of Ceramics," Proceedings of the First International Conf. on Fracture, Sendai, Japans, 3, 1307-1320 (1965).

12. Wright, W., and Byrne, J. G., "Stress Concentrations in Concrete," Nature, 203, 1374-1375 (1964).

13. Durelli, A. J., and Parks, V., "Relationship of Size and Stress Gradient to Brittle Fracture Stress," Proc. Fourth U. S. National Nat. Cong. Appl. Mech., 2, 931-938 (1962).

14. Juvinall, R. C., Stress, Strain and Strength, McGraw Hill Book Co., New York, p. 231 (1967).

15. Gilman, J. J., and Tuler, F. R., "Dynamic Fracture by Spallation in Metals," Int. Journal of Fracture Mech., 6, No. 2, 169-182 (1970).

16. Peck, J. C., Berkowitz, H. M., and Cohen, L. J., "The Relationship of the Critical Stress Versus Impulse Theory of Spall Fracture to the Stress Gradient Theory," Int. Journal of Fracture Mech., 5, No. 4, 297-303 (1969).

17. Brown, W. S., and Swanson, S. R., "Constitutive Equations for Westerly Granite and Cedar City Tonalite for a Variety of Loading Conditions," Final Report, DASA-2473, University of Utah, March 70.

18. Brown, W. S., and Swanson, S. R., "Stress-Strain and Fracture Properties of Nugget Sandstone," Final Report, AFWL-7R-71-54, University of Utah, March 71.

19. Swanson, S. R., and Brown, W. S., "The Influence of State of Stress on Stress-Strain Behavior of Rocks," ASME Paper No. 71-Met-AA (1971).

20. Brown, W. S., Swanson, S. R., and Wawersik, W. R., "Influence of Dynamic Loading, Biaxial Loading, and Pre-Fracturing on the Stress-Strain and Fracture Characteristics of Rocks," Final Report, DASA-2713, University of Utah, March 71.

21. Brown, W. S., Swanson, S. R., and Wawersik, W. R., "Further Studies of Dynamic and Biaxial Loading of Rock," Final Report, UTEC ME 72-015, University of Utah, in publication (1972).

22. Wawersik, W. R., and Brown, W. S., "Creep Fracture in Rock in Uniaxial Compression," Final Report, UTEC ME 71-242, University of Utah, December 1971.

23. Brace, W. F., Paulding, B. W., and Scholz, C., "Dilatancy in the Fracture of Crystalline Rocks," J. Geophys. Res., 71, 3939-3953 (1966).

24. Birch, F., "The Velocity of Compressional Waves in Rocks to 10 Kilobars, Part 1," J. Geophys. Res., 65, 1083-1102 (1960).

25. Wawersik, W. R., "Detailed Analysis of the Rock Fracture in Laboratory Compression Tests," Ph.D. Thesis, University of Minnesota (1968).

26. Brown, W. S., and Swanson, S. R., "Influence of Load Path and Stress on Failure Strength and Stress-Strain Properties of Rock," Technical Report AFWL-TR-70-53, University of Utah, April 70.

27. Swanson, S. R., and Brown, W. S., "An Observation of Loading Path Independence of Fracture in Rock," Int. J. Rock Mech., Min. Sci., 8, 277-281 (1971).

28. Mogi, K., "Effect of Intermediate Principal Stress on Rock Failure," J. Geophys, Res., 72, 5117-5137 (1967).

29. Neuber, H., "Theory of Notch Stresses: Principles of Exact Stress Calculation," J. W. Edwards, Publisher, Inc., Ann Arbor, Mich., (1946).

30. Weibull, W., "The Phenomenon of Rupter in Solids," Ingeniors Vetenskaps Akademien, Handlinger, No. 153 (1939).

31. Williams, M. L., "On the Stress Distributions at the Base of a Stationary Crack," J. of Applied Mechanics, 109-114, (1957).

32. Paris, P. C., and Sih, G. C., "Stress Analysis of Cracks," Fracture Toughness Testing and Its Applications, ASTM STP No. 381 (1965).

33. Swanson, S. R., "Finite Element Solutions for a Cracked Two Layered Elastic Cylinder," Engineering Fracture Mechanics, 3, 283-289 (1971).

34. Williams, J. G., and Constable, I., "Some Observations on K_{1c} Determination for Round Bars in Tension and Bending," Int. J. of Fracture Mech., 5, No. 2 (1969).

35. Irwin, G. R., "Crack-Toughness Testing of Strain-Rate Sensitive Materials," Trans. ASME, J. of Eng. for Power, 86, 444-450 (1964).

36. Brace, W. F., and Walsh, J. B., "Some Direct Measurements of the Surface Energy of Quartz and Orthoclase," The American Mineralogist, 47, 1111-1122 (1962).

37. Santhanam, A. T., and Gupta, Y. P., "Cleavage Surface Energy of Calcite," Rock Mech., Min. Sci., 5, 253-259 (1968).

38. Bieniawski, Z. T., "Fracture Dynamics of Rock," The Int. J. of Fracture Mech., 4, 415-430 (1968).

39. Perkins, T. K., and Bartlett, L. E., "Surface Energies of Rocks Measured During Cleavage," Soc. Pet. Eng. Jour., 3, 307-313, (1963).

40. Perkins, T. K., and Krech, W. W., "Effect of Cleavage Rate and Stress Level on Apparent Surface Energies of Rocks," Soc. Pet. Eng. Jour., 6, 308-314 (1966).

41. Weiss, V., Schaeffer, G., and Fehling, J., "Effect of Section Size on Notch Strength," ASME J. Basic Eng., 88, 675-681 (1966).

42. Weiss, V., "Application of Weibull's Statistical Theory of Fracture to Sheet Specimens," ASME paper No. 62-WA-270 (1962).

43. Weiss, V., and Yukawa, S., "Critical Appraisal of Fracture Mechanics," Fracture Toughness Testing and Its Applications, ASTM STP No. 381 (1965).

Table 1. Tension Test Results

Specimen No.	Notch	Net Section Stress-psi	Nominal Dia.-in.
	Westerly		
6	Smooth	1260	1
101	Smooth	1190	3/4
115	Smooth	1935	1
116	Smooth	1745	1
3-2	1/8	1470	2
2	1/8	1256	1
99	1/32	1090	1
1-2	1/32	1370	2
4	.0015	1196	1
2-2	.0015	1340	2
	Nugget		
7	Smooth	518	1
12	Smooth	455	1
13	Smooth	700	1
14	Smooth	706	1
102	Smooth	830	3/4
11-2	Smooth	732	2
117	Smooth	733	1
6-2	1/8	576	2
8	1/8	527	1
88	1/32	635	1
4-2	1/32	553	2
110	.0015	535	1
111	.0015	442	1
5-2	.0015	538	2
	Marble		
89	Smooth	885	3/4
90	Smooth	735	3/4
91	Smooth	928	3/4
12-2	Smooth	1260	2
118	T-17	1013	1
9-2	1/8	1260	2
100	1/8	1310	1
7-2	1/32	1110	2
95	1/32	1140	1
96	.0015	1240	1
8-2	.0015	1060	2

Table 2. Tension Tests for Nugget Sandstone, Block 2

Specimen No.	Nominal O.D. in.	Notch Radius in.	Notch Depth in.	Net Section Stress-psi	Outside Diameter D-in.	Diameter at Notched Section d-in.
0-47	1	Smooth	Smooth	1310		
0-58	1	Smooth	Smooth	1110		
0-59	1	Smooth	Smooth	1270		
0-60	1	Smooth	Smooth	1120		
0-9	1	Smooth	Smooth	1070		
0-10	1	Smooth	Smooth	1500		
0-11	1	Smooth	Smooth	1260		
0-61	1	.0015	1/16	695	0.972	0.850
0-62	1	.0015	1/16	666	0.960	0.826
0-63	1	.005*	1/8	691	0.940	0.723
0-64	1	.005*	1/4	697	0.950	0.452
0-65	1	.0015	1/4	757	0.970	0.475
0-66	1	.0015	1/8	564	0.920	0.682
0-67	1	.0015	3/16	592	0.971	0.586
0-68	1	.0015	3/16	556	0.906	0.535
0-69	1	.004	1/4	726	0.975	0.497
0-70	1	.004	1/8	622	0.973	0.720

Table 3. Extension Test Results (All 1")

Notch Type	Confining Pressure-ksi	Westerly Granite Spec. No.	Westerly Granite Net Section Stress-psi	Nugget Sandstone Spec. No.	Nugget Sandstone Net Section Stress-psi	Tennessee Marble Spec. No.	Tennessee Marble Net Section Stress-psi
Smooth	5	113	7760	114	7590		
		52	6145	50	5603	112	6610
	10	84	11800	98	12300	109	11700
		51	10250				
	15			11	13315		
	20	85	22900	97	22900	106	23300
	30	86	30800	94	31800	105	31800
1/8	5	8	6120	13	6200		
		16	6990				
	10	38	12500	14	10900	60	11800
	20	41	18900	7	18400	59	21600
	30	39	28200	43	31100	58	30000
		53	26800	44	26000		
				45	28800		
1/32	5	28	5170	27	6390		
	10	18	10500	55	11300	64	10600
				22	11000		
	20	77	18500	80	19400	63	20300
				24	18100		
	30	78	21700	81	26000	62	22600
				25	25300		
	22.2	21	24100				
0.0015	5	15	6100	9	4740		
	10	48	11500	35	10900	68	11100
		54	13680	75	9690		
				32	11200		
	20	10	16800	36	20500	104	21500
				33	17400	67	9240
	30	76	21400	37	29300	66	22600
				34	22200		

Table 4. Torsion Test Results

Specimen Configuration	Westerly Granite			Nugget Sandstone			Tennessee Marble		
	Spec. No.	Max. Torque in-lb	Net Sect. $\tau = \frac{Tc}{J}$ psi	Spec. No.	Max. Torque in-lb	Net Sect. $\tau = \frac{Tc}{J}$ psi	Spec No.	Max. Torque in-lb	Net Sect. $\tau = \frac{Tc}{J}$ psi
Smooth	12	736	3750	7	408	2080	70	527	2680
				8	416	2120			
				9	442	2250			
Circumferential, 1/8	14	454	5592	11	234	2870	71	491	4920
1/32	47	582	7030	23	425	5130	73	482	5820
.0015	13	500	5471				72	529	6390
Longitudinal, 1/8	15	625		16	478				

Table 5. Bending Test Results

Rock Type	Spec. No.	Specimen Dimensions b=in.	h=in.	Max. Load lbs	Bending Moment in-lb	Bending Stress psi
Tennessee Marble	B-1	1.003	0.497	104	78.0	1890
	B-2	1.010	0.538	128	96.0	1970
	B-3	1.005	0.510	117	87.7	2014
Westerly Granite	B-4	1.050	0.564	286	214.5	3853
	B-5	1.058	0.508	222	166.5	3659
	B-6	1.047	0.493	197	147.7	3484
	B-7	1.050	0.497	210	157.5	3644
Nugget Sandstone	B-8	1.025	0.535	121	91.8	1877
	B-9	1.018	0.520	108	81.4	1775
	B-10	1.027	0.522	127	95.1	2040
	B-11	1.026	0.753	240	180.0	1856

Table 6. Stress Concentration Factors Obtained from the Finite Element Analyses of the Notched Cylindrical Bars

Notch Radius (inch)	K_t, Axial Stress Concentration Factor	
	1" Diameter Bar	2" Diameter Bar
1/8	2.06	2.52
1/32	3.58	4.40
0.0015	14.66	18.03

Table 7. K_{1c} Values Calculated from 0.0015 Tip Radius Specimen Tests

Rock	Specimen No.	K_{1c} $psi\sqrt{in.}$	$\delta = \frac{1}{2\pi}\left(\frac{K_{1c}}{\sigma_{TS}}\right)^2$ inch
Westerly granite	4	545	.0118
Westerly granite	2-2	769	.0235
Nugget sandstone	110	244	.0155
Nugget sandstone	111	202	.0106
Nugget sandstone	5-2	309	.0249
Tennesse marble	96	565	.0320
Tennesse marble	8-2	608	.0371

Table 8. Fracture Energy (γ_F) Values

Material	γ in-lbs/in^2	Reference
Westerly Granite	0.097	Present study; from K_{1c} = 657 psi $\sqrt{in}$
Nugget Sandstone	0.011	Present study; from K_{1c} = 252 psi $\sqrt{in}$
Tennessee Marble	0.068	Present study; from K_{1c} = 587 psi $\sqrt{in}$
Tennessee Marble II	0.22	Wawersik (27), Nominal crack area
	0.056	Wawersik (27), Measured crack area
Charcoal Gray Granite II	0.38	Wawersik (27), Nominal crack area
	0.089	Wawersik (27), Measured crack area
Quartz	0.00234 to 0.00589	Brace and Walsh (36); Values depend on orientation
Orthoclase	0.0444	" " "
Calcite	0.00198	Santhanam and Gupta (37)
Quartzite	1.75	Bieniawski (38)
Norite	2.10	Bieniawski (38)
Arizona Sandstone	0.78	Perkins and Bartlett (39)
Milsap Sandstone	0.65	Perkins and Bartlett (39)
Colorado Sandstone	0.55	Perkins and Bartlett (39)
Woodbine Sandstone	0.054	Perkins and Bartlett (39)
Torpedo Sandstone	0.35	Perkins and Bartlett (39)
Boise Sandstone	0.25	Perkins and Bartlett (39)
Austin Limestone	0.044	Perkins and Bartlett (39)
Carthage Limestone	0.22	Perkins and Bartlett (39)
Leuders Limestone	0.11	Perkins and Bartlett (39)
Indiana Limestone	0.24	Perkins and Bartlett (39)

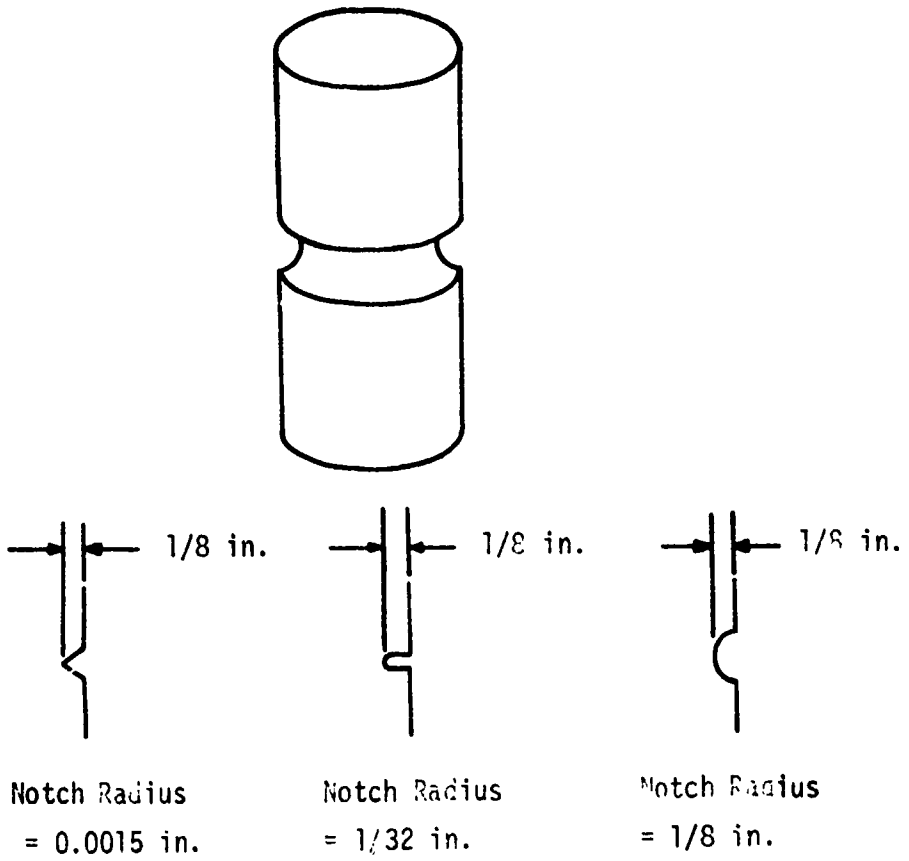

Figure 1. Notched Rock Specimens

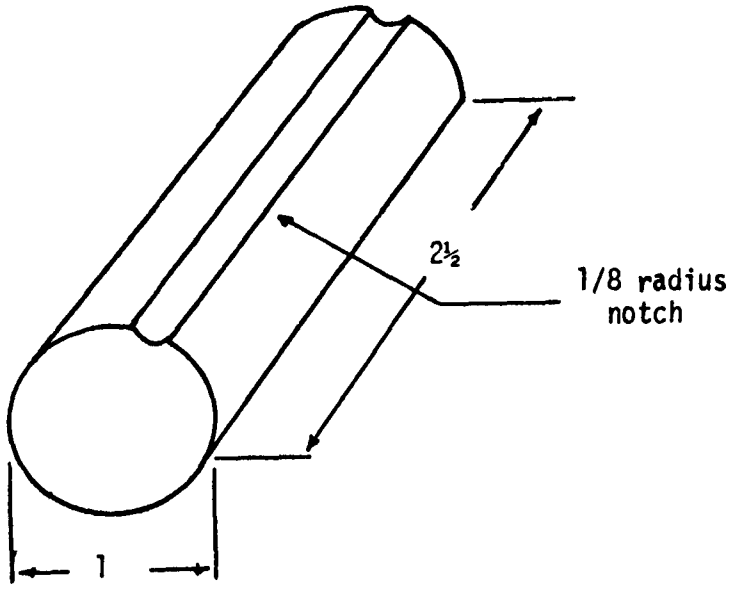

FIGURE 2. Torsion specimen with longitudinal notch.

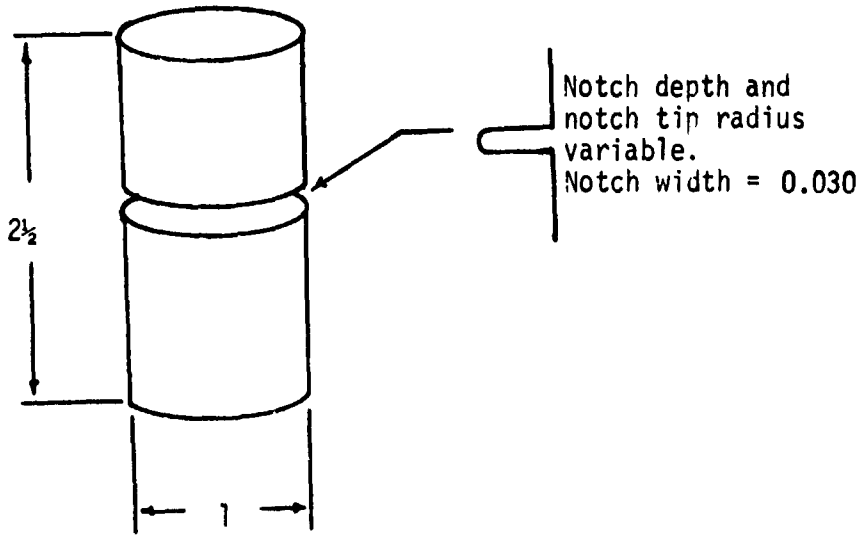

FIGURE 3. Notched specimens used in Nugget sandstone Block II tension tests.

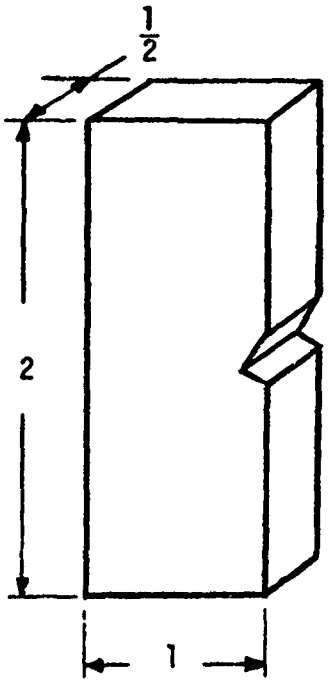

FIGURE 4. Notched compression specimen.

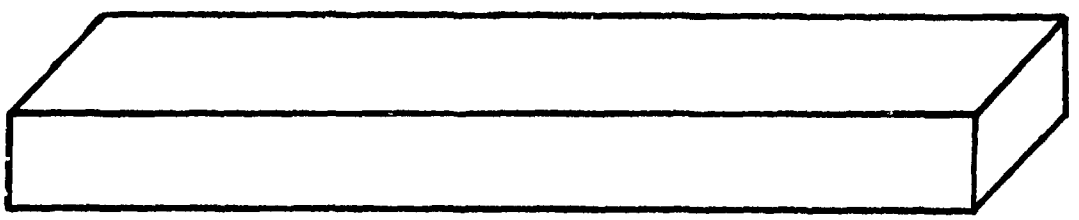

FIGURE 5. Bend test specimen.

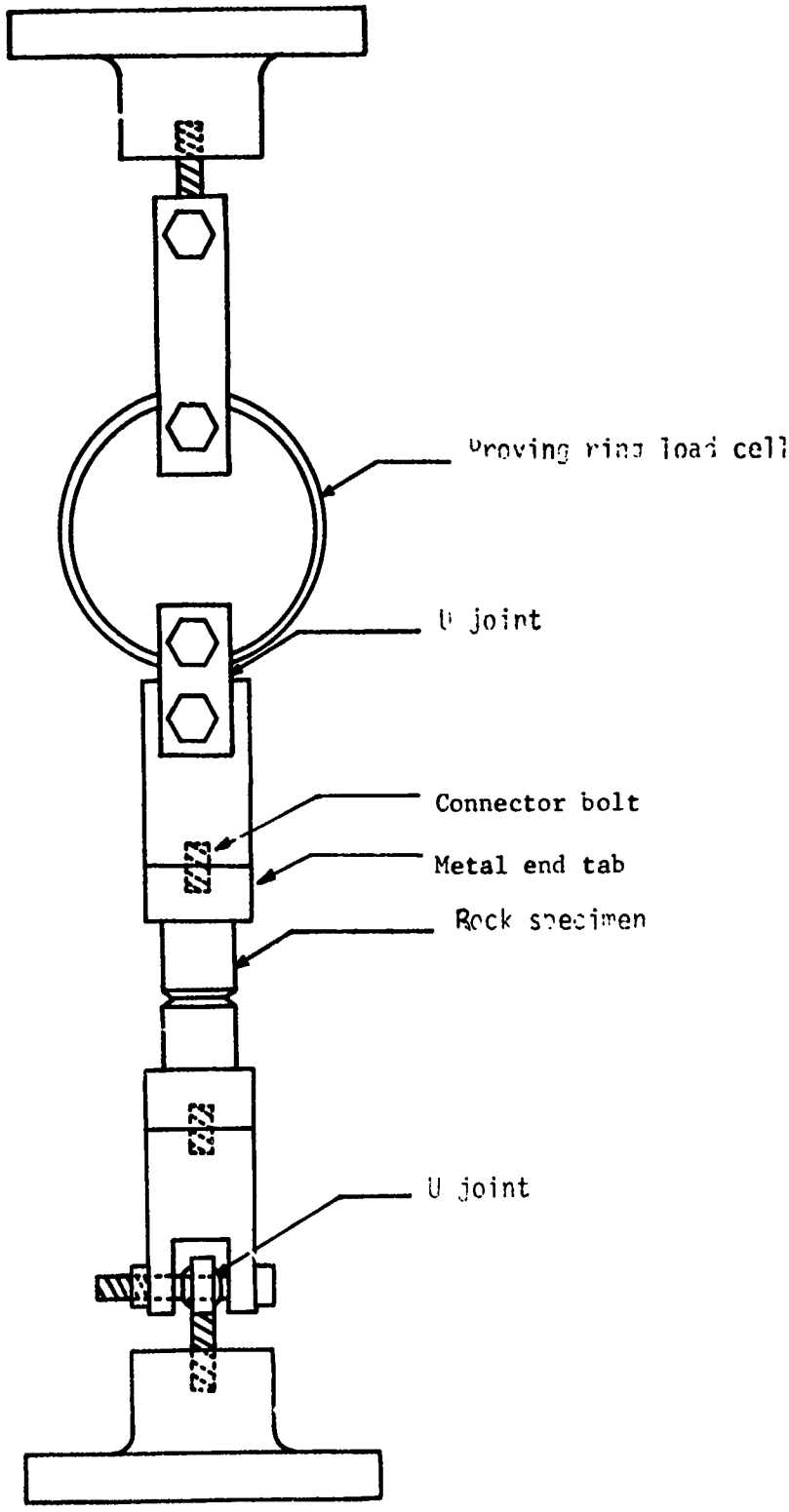

Figure 6. Schematic of Tension Test Apparatus

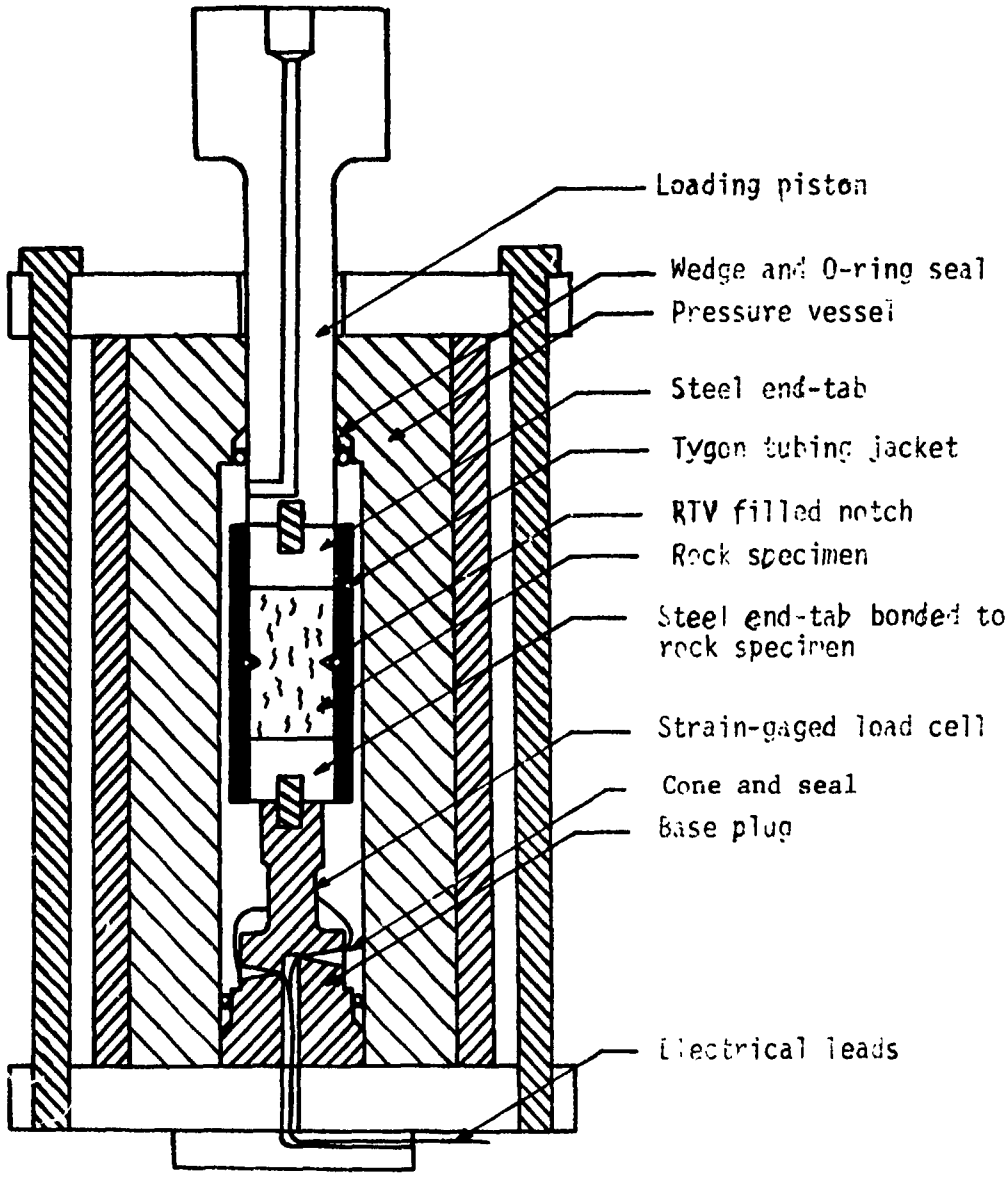

Figure 7. Schematic of extension apparatus

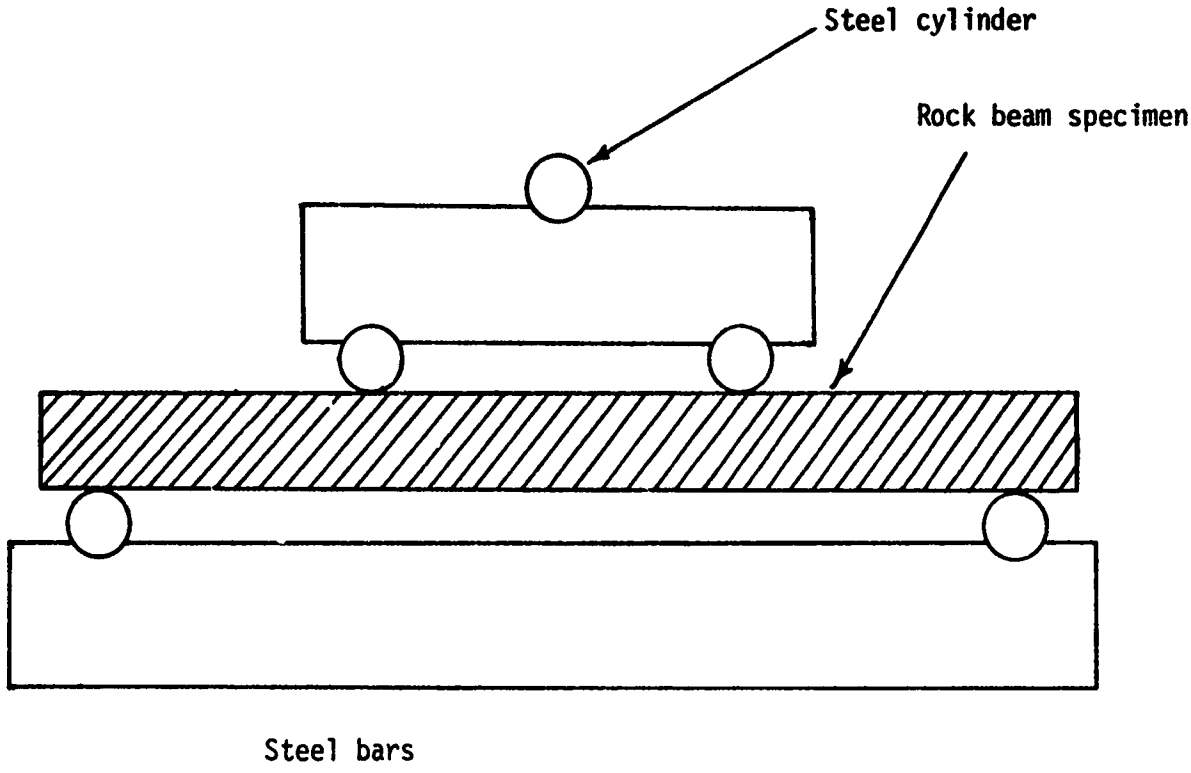

FIGURE 8. Beam bending test apparatus.

Westerly Granite No. 2, 1/8 Notch

Nugget Sandstone No. 1, 1/8 Notch

Tennessee Marble No. 89, Unnotched

FIGURE 9. Fracture surface of tension specimens.

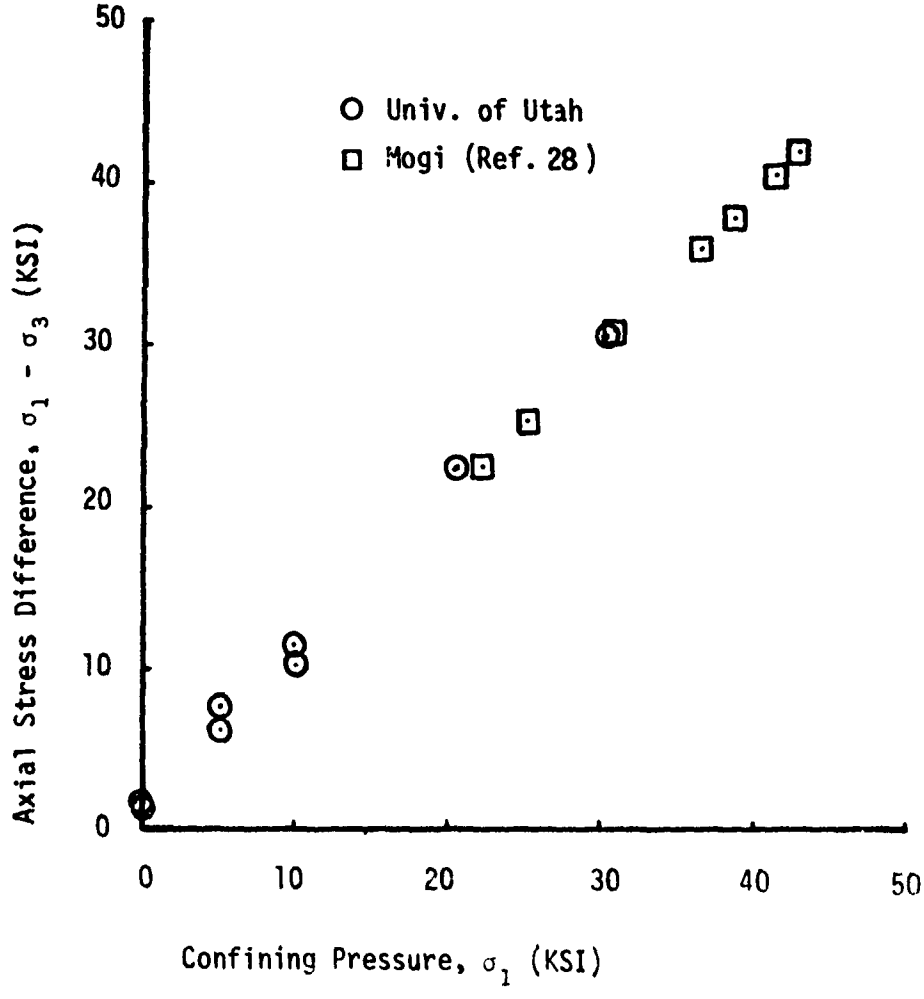

Figure 10. Tension and Extension Test Results for Westerly Granite (Unnotched)

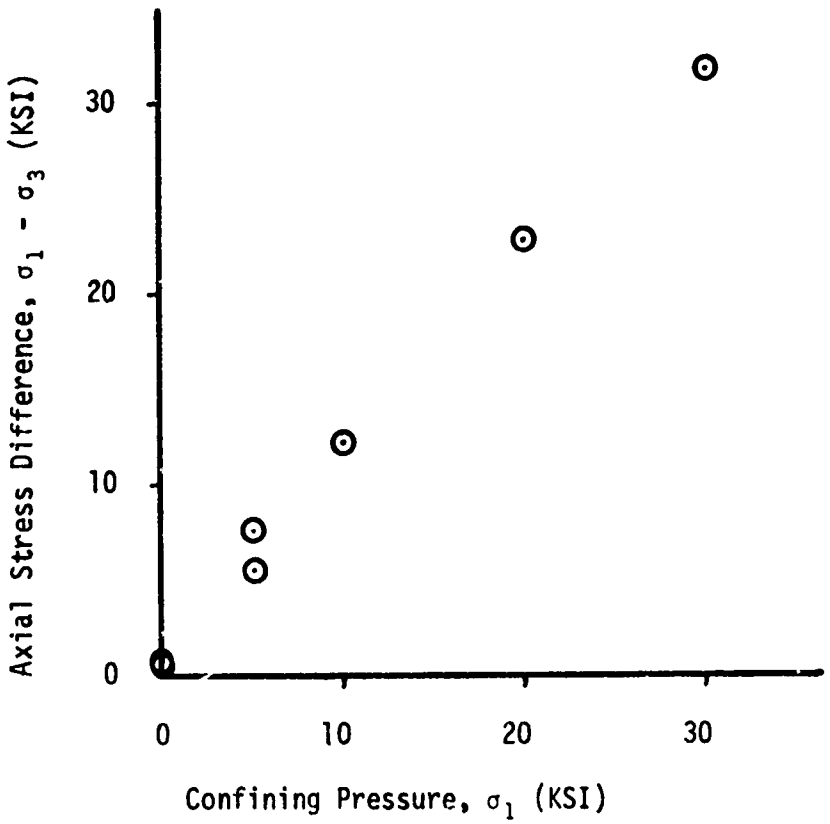

Figure 11. Tension and Extension Test Results for Nugget Sandstone (Unnotched)

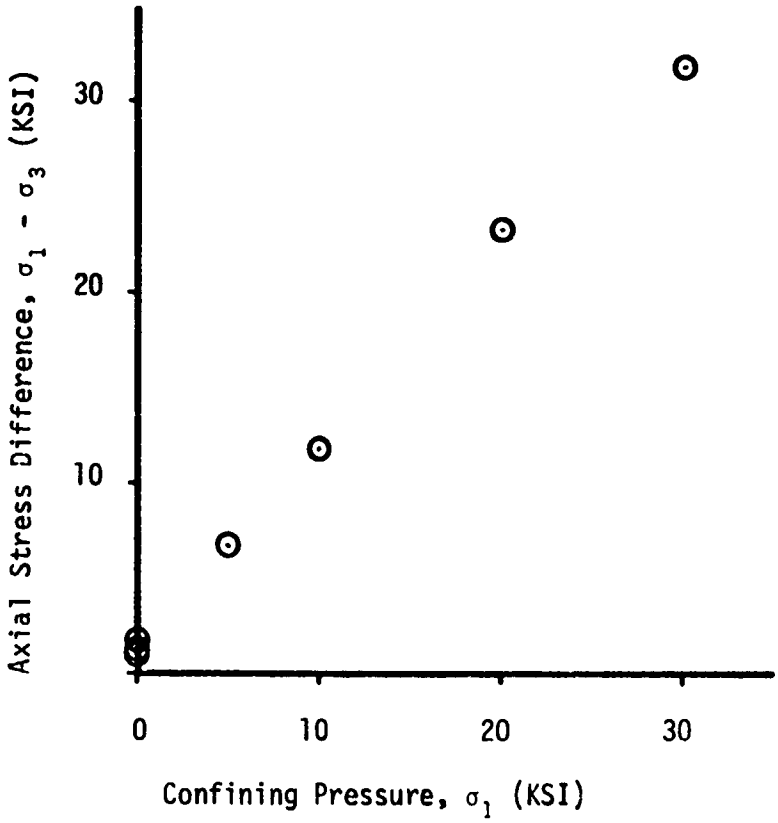

Figure 12. Tension and Extension Test Results for Tennessee Marble (Unnotched)

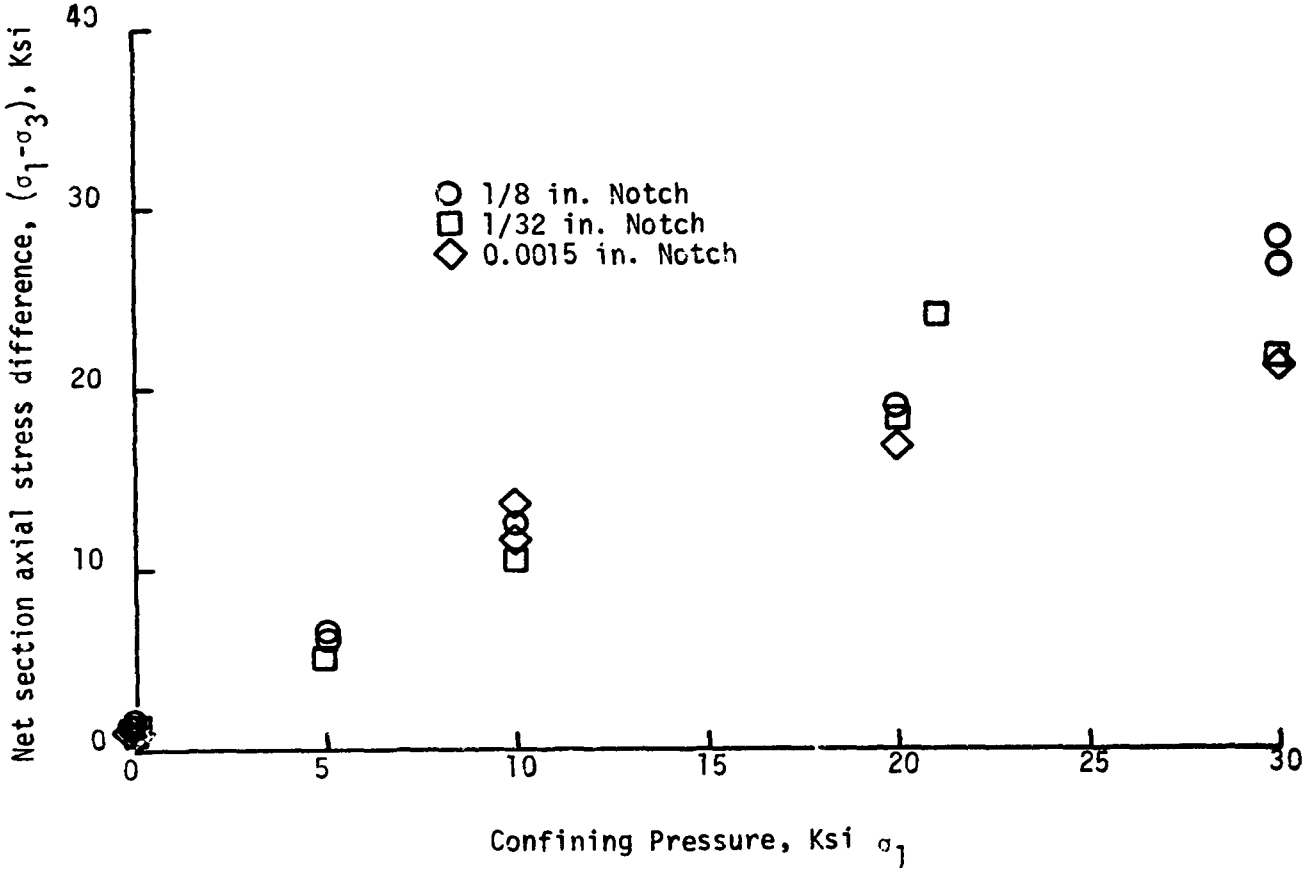

FIGURE 13. Extension test results for notched Westerly granite specimens.

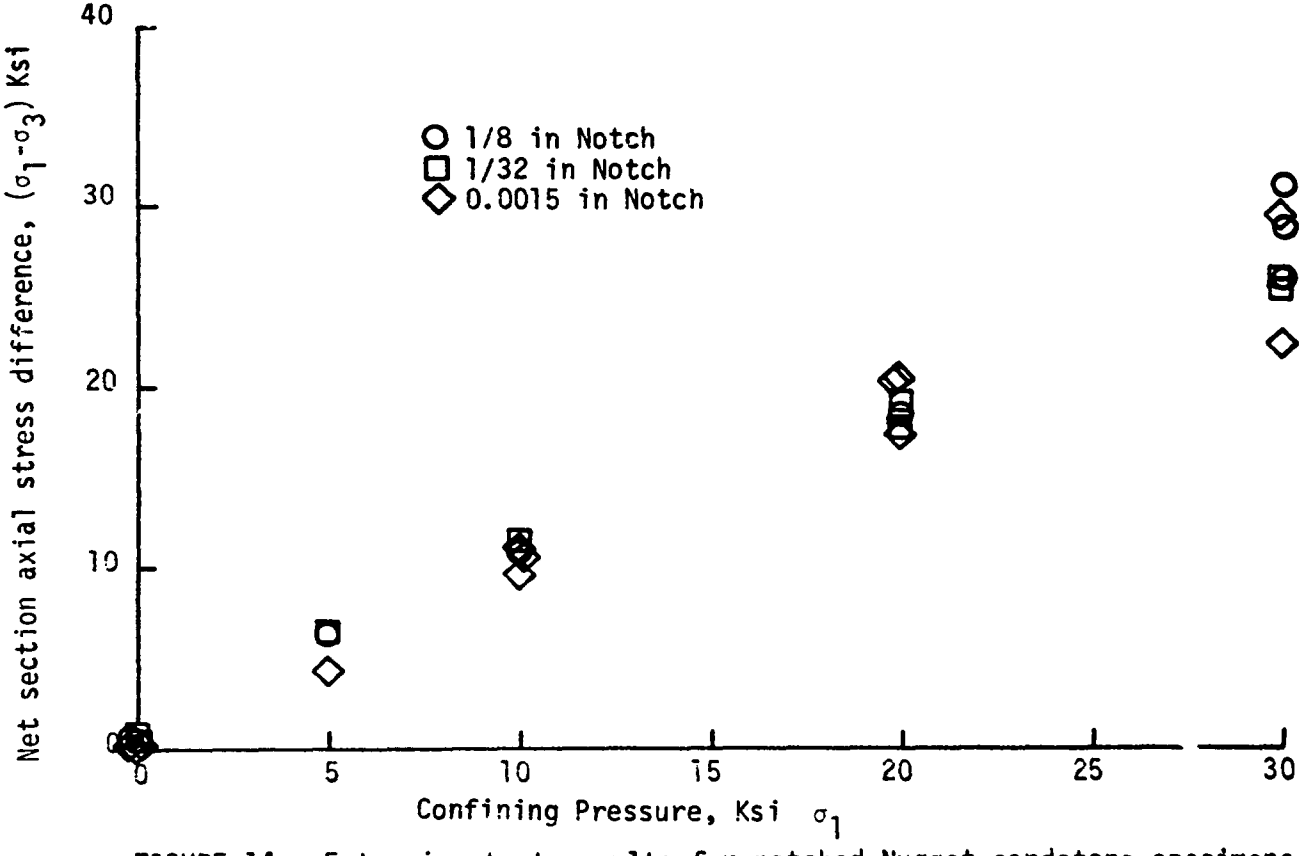

FIGURE 14. Extension test results for notched Nugget sandstone specimens.

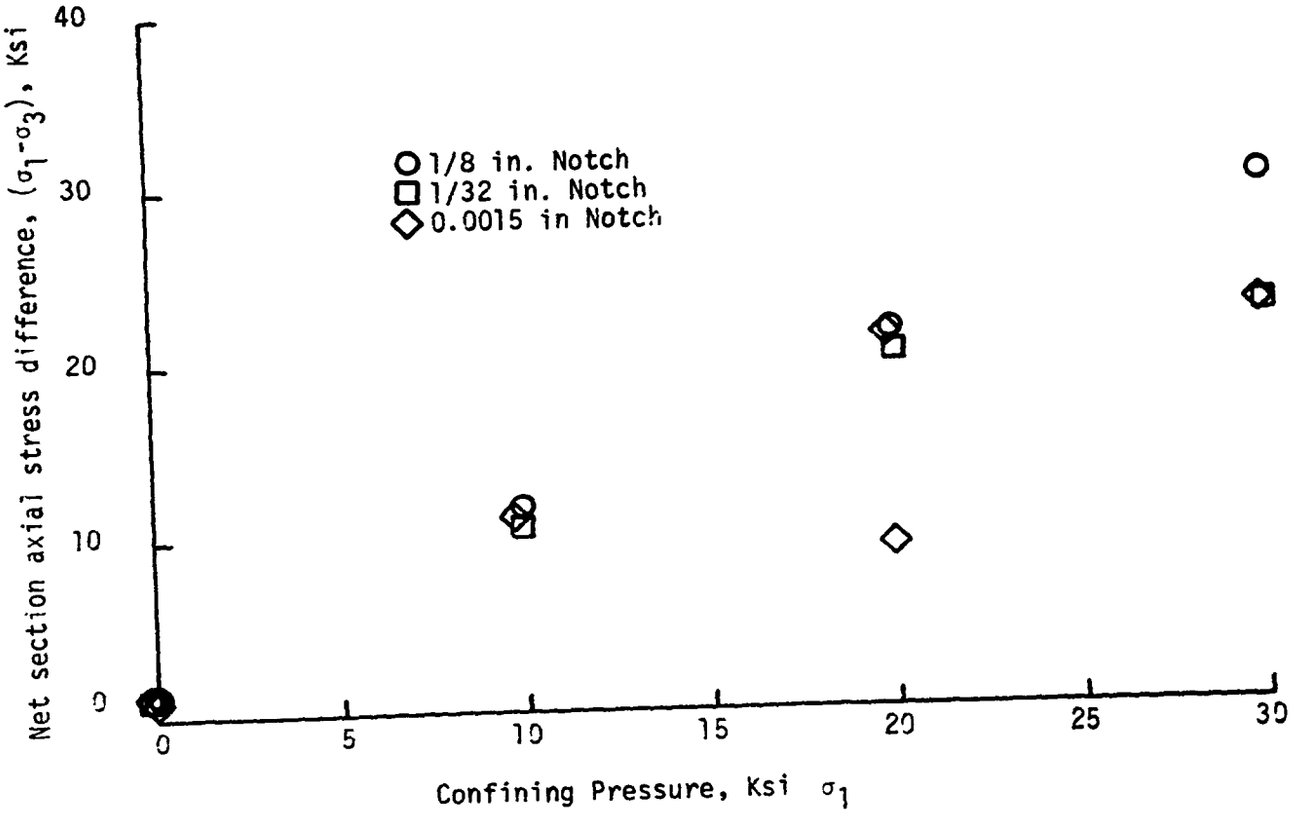

FIGURE 15. Extension test results for notched Tennessee marble specimens.

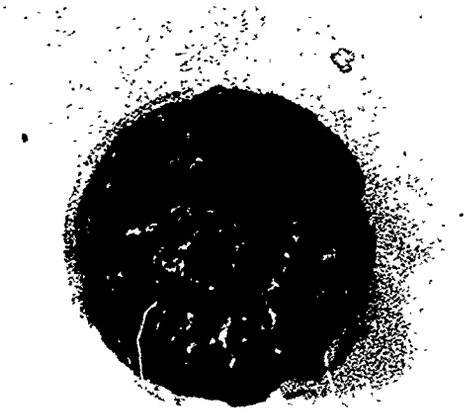

Tennessee Marble No. 59, 1/8 Notch

Westerly Granite No. 51,
Unnotched

Nugget Sandstone No. 45,
1/8 Notch

FIGURE 16. Fracture surface of extension specimens.

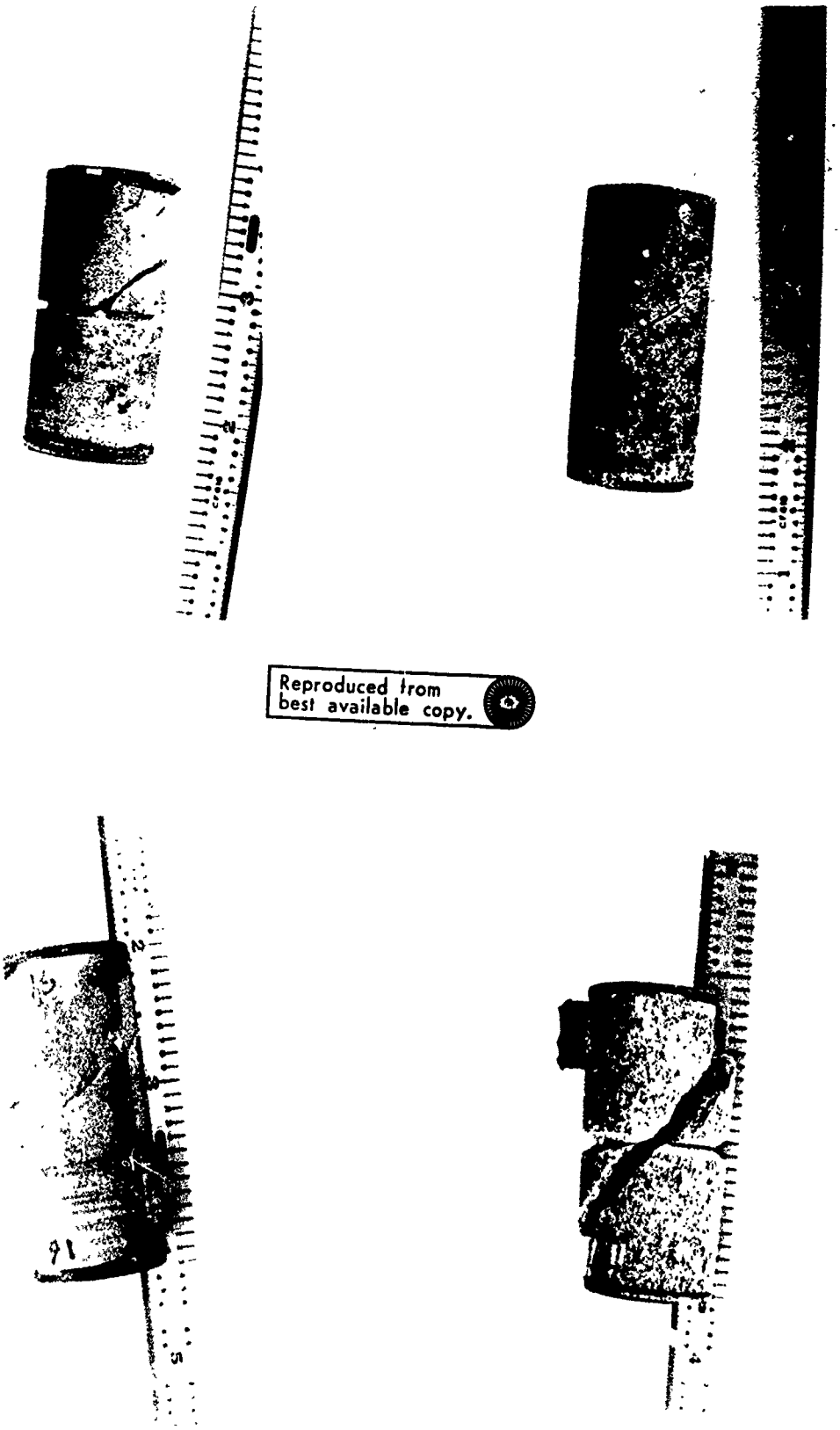

FIGURE 17. Fractured torsion specimens.

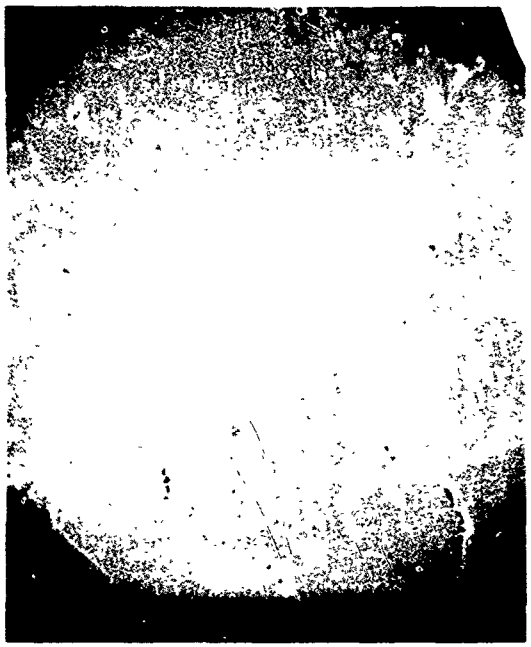

Neutral Axis 250X

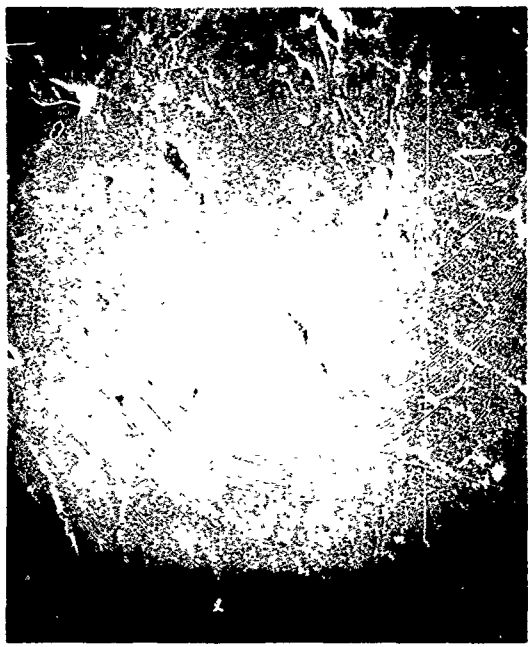

Tension Side 250X

Tension Side 2500X

FIGURE 18. Scanning electron microscope photo of Westerly Granite beam section.

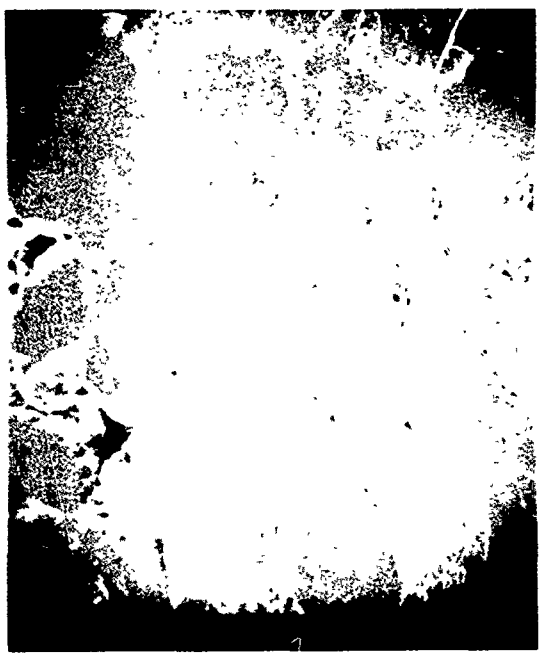

Neutral Axis 235X

Tension Side 240X

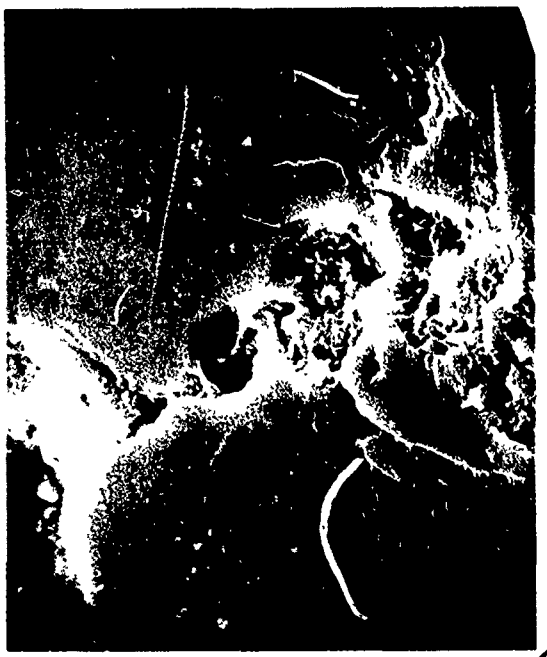

Tension Side 2400X

FIGURE 19. Scanning electron microscope photo of Nugget Sandstone beam section.

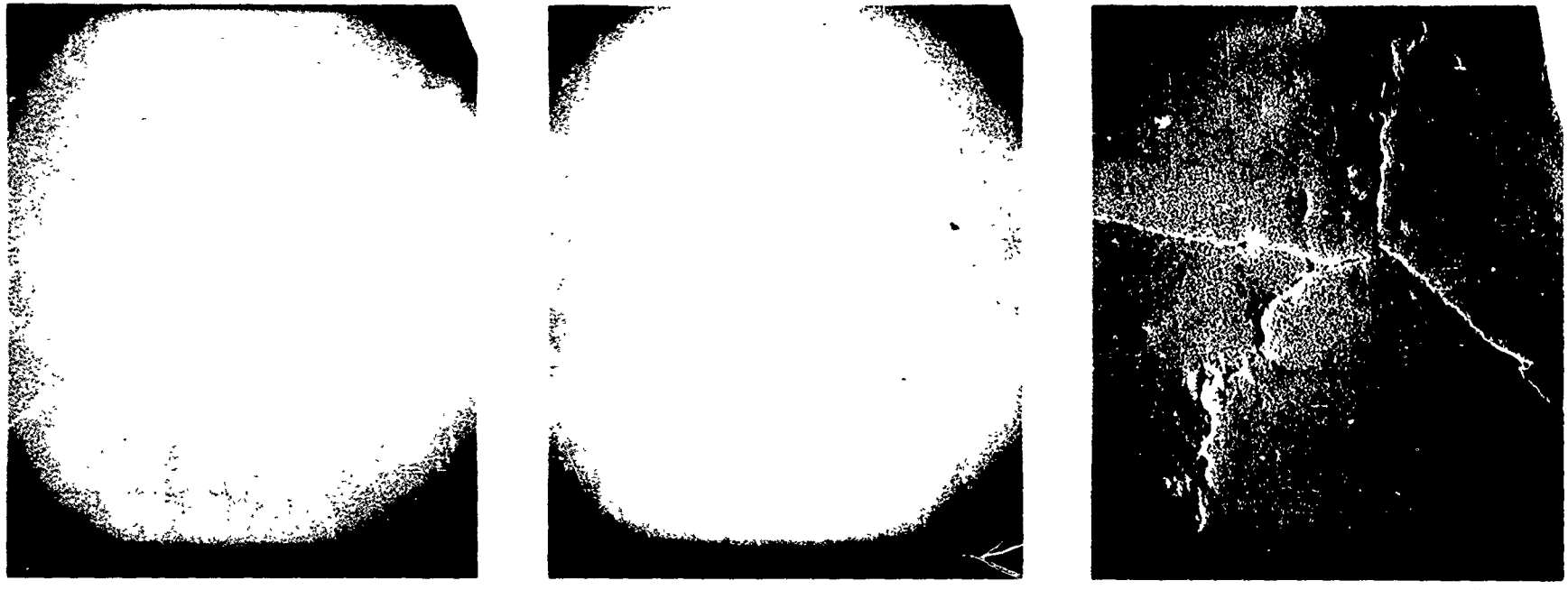

Neutral Axis 240X

Tension Side 240X

Tension Side 2400X

FIGURE 20. Scanning electron microscope photo of Tennessee Marble beam section.

FIGURE 21. Notched compression test fractures.

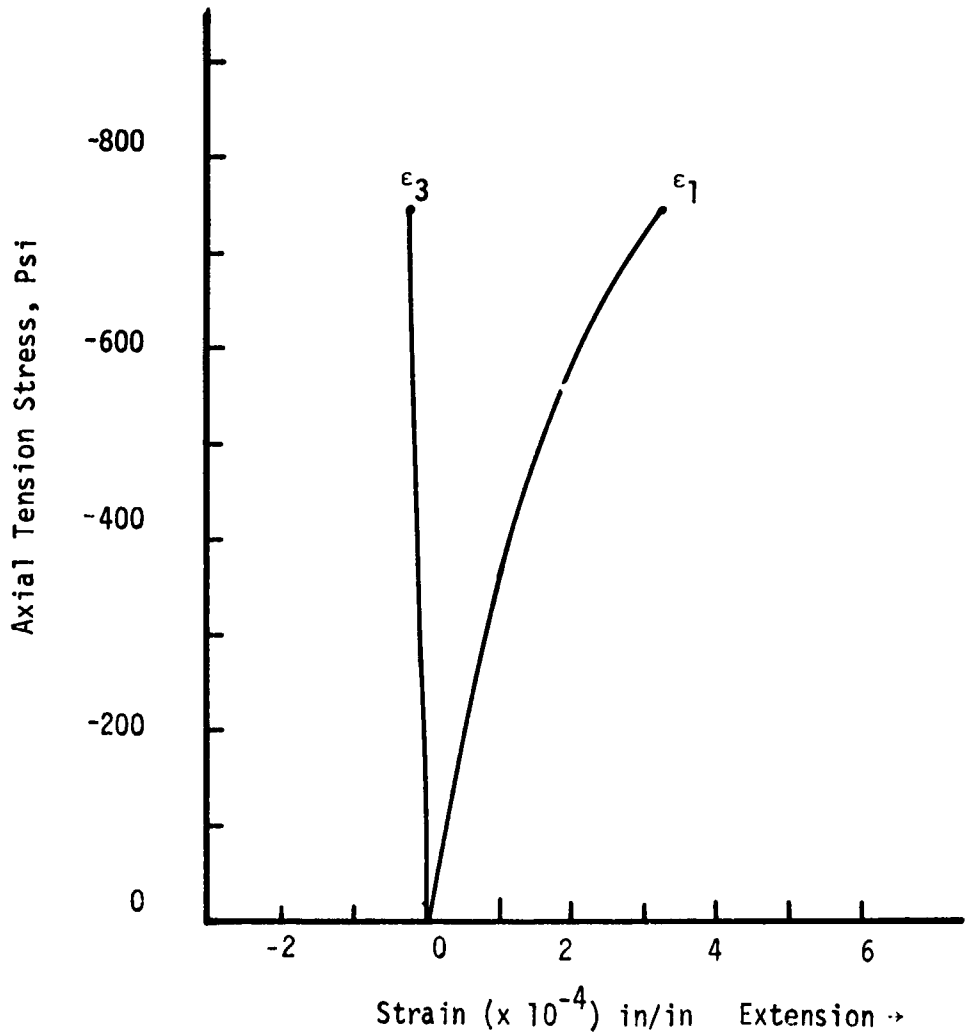

FIGURE 22. Principal stress-strain curves for tension test of Westerly granite. (From Reference 18)

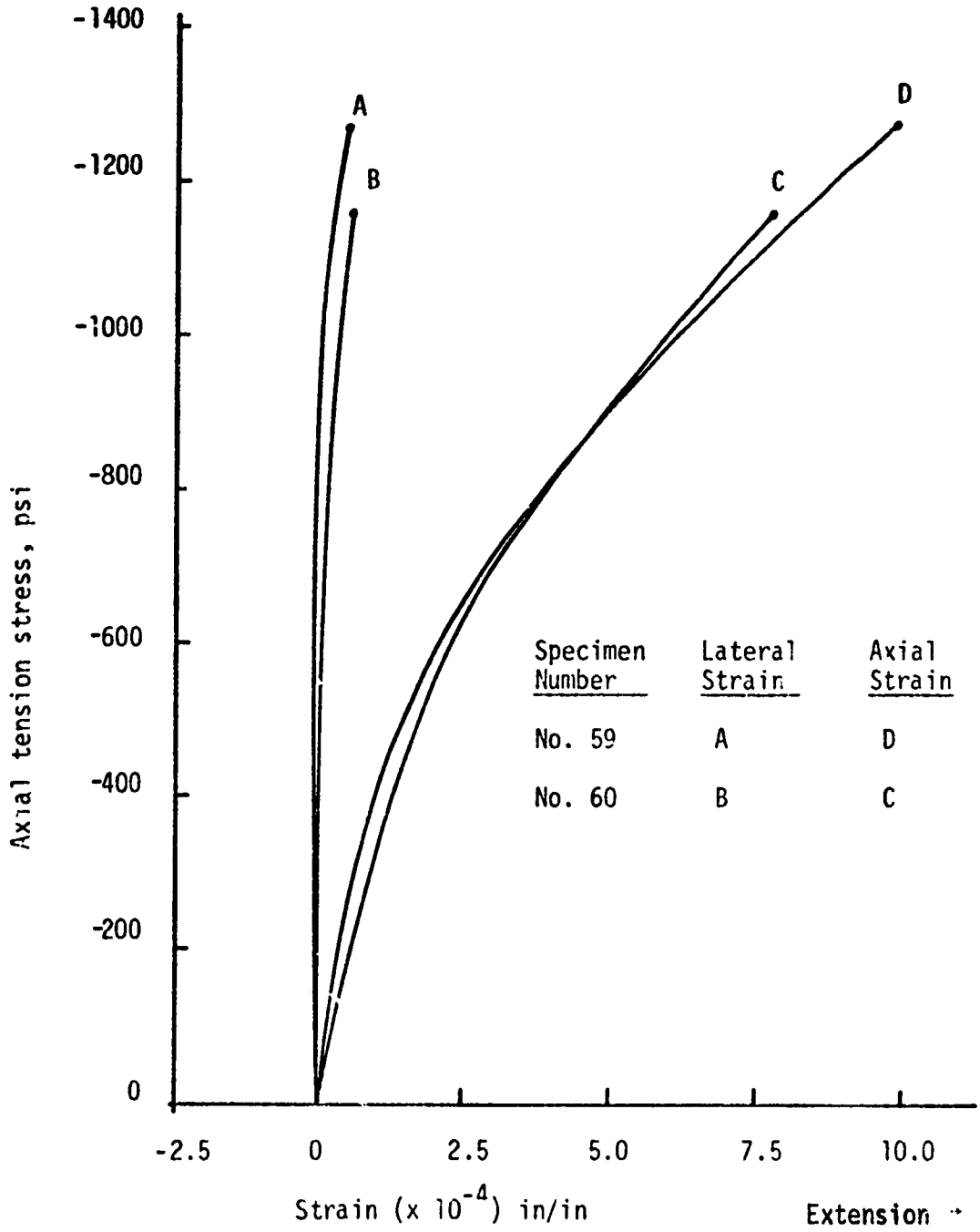

Figure 23. Principal stress-strain curve for tension test of Nugget sandstone specimens. (From Reference 18)

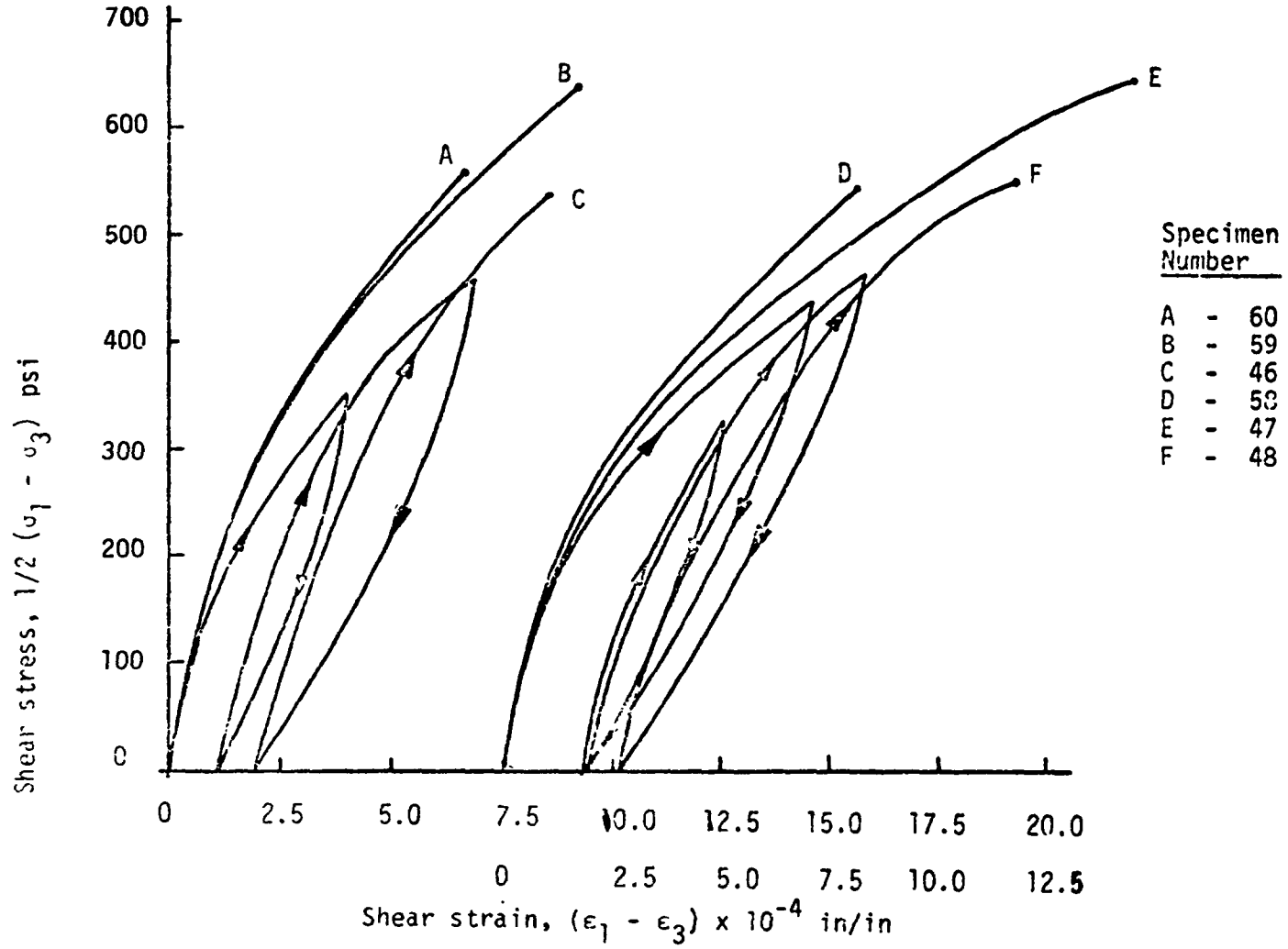

Figure 24. Shear stress-strain curves in unconfined tension tests of Nugget sandstone. (From Reference 18)

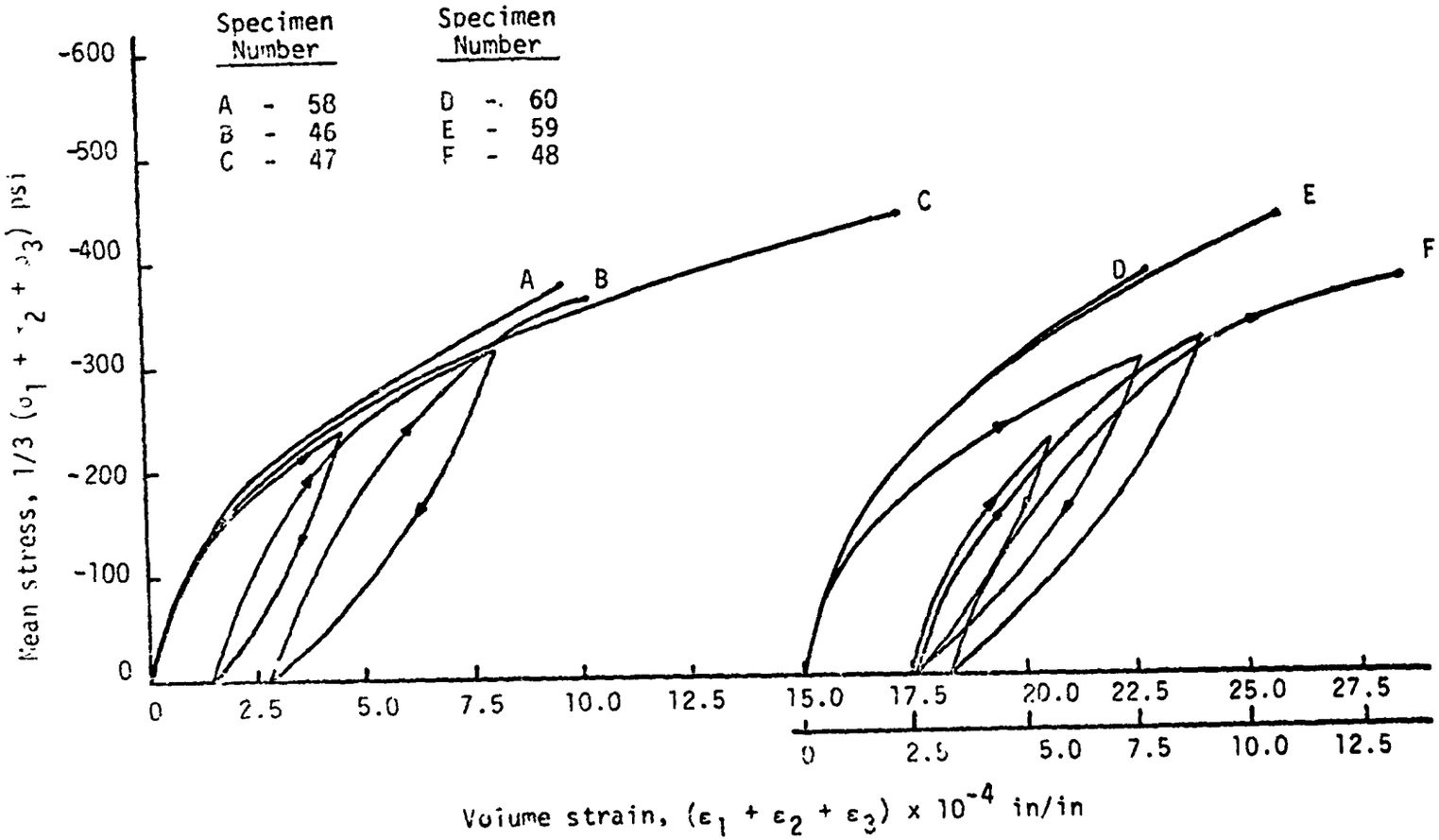

Figure 25. Dilatation stress-strain curves in unconfined tension tests of Nugget sandstone. (From Reference 18)

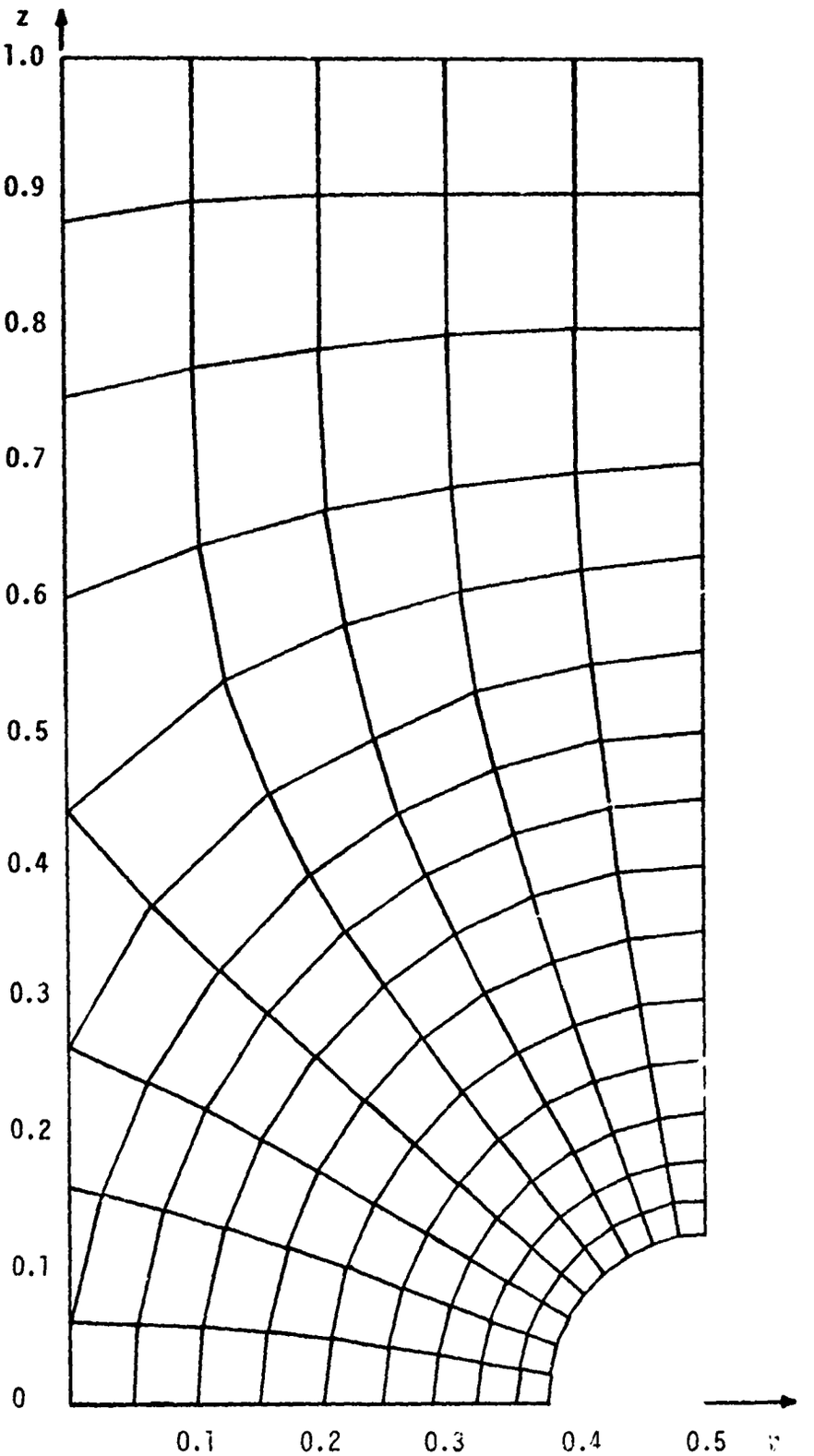

Figure 26. Finite-element Grid for 1/8 in. Radius Notched Test Specimen.

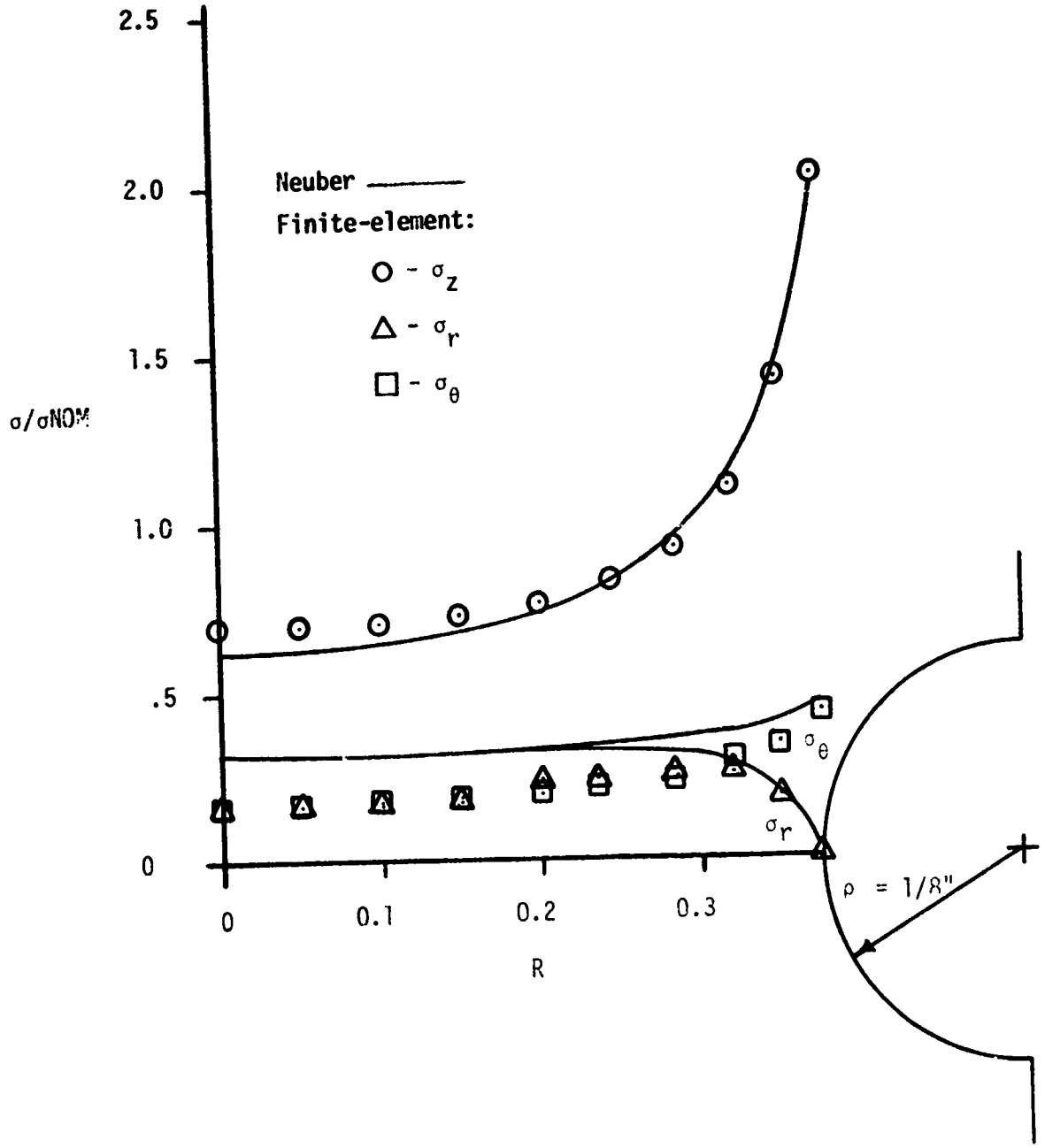

Figure 27. Comparison of Finite-element Results with Neuber Solution in Vicinity of 1/8 in. Radius Notch

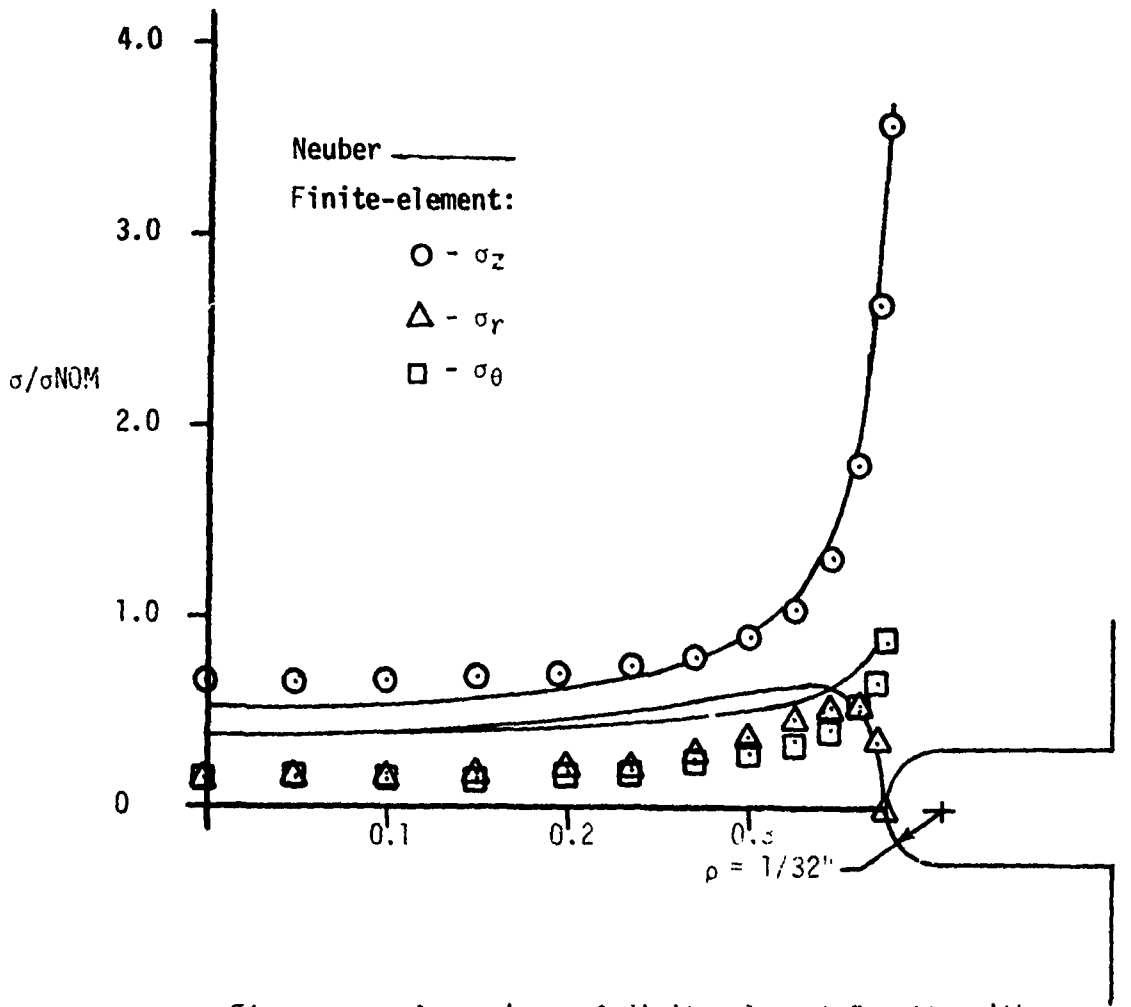

Figure 28. Comparison of Finite element Results with Neuber Solution in Vicinity of 1/32 in. Radius Notch

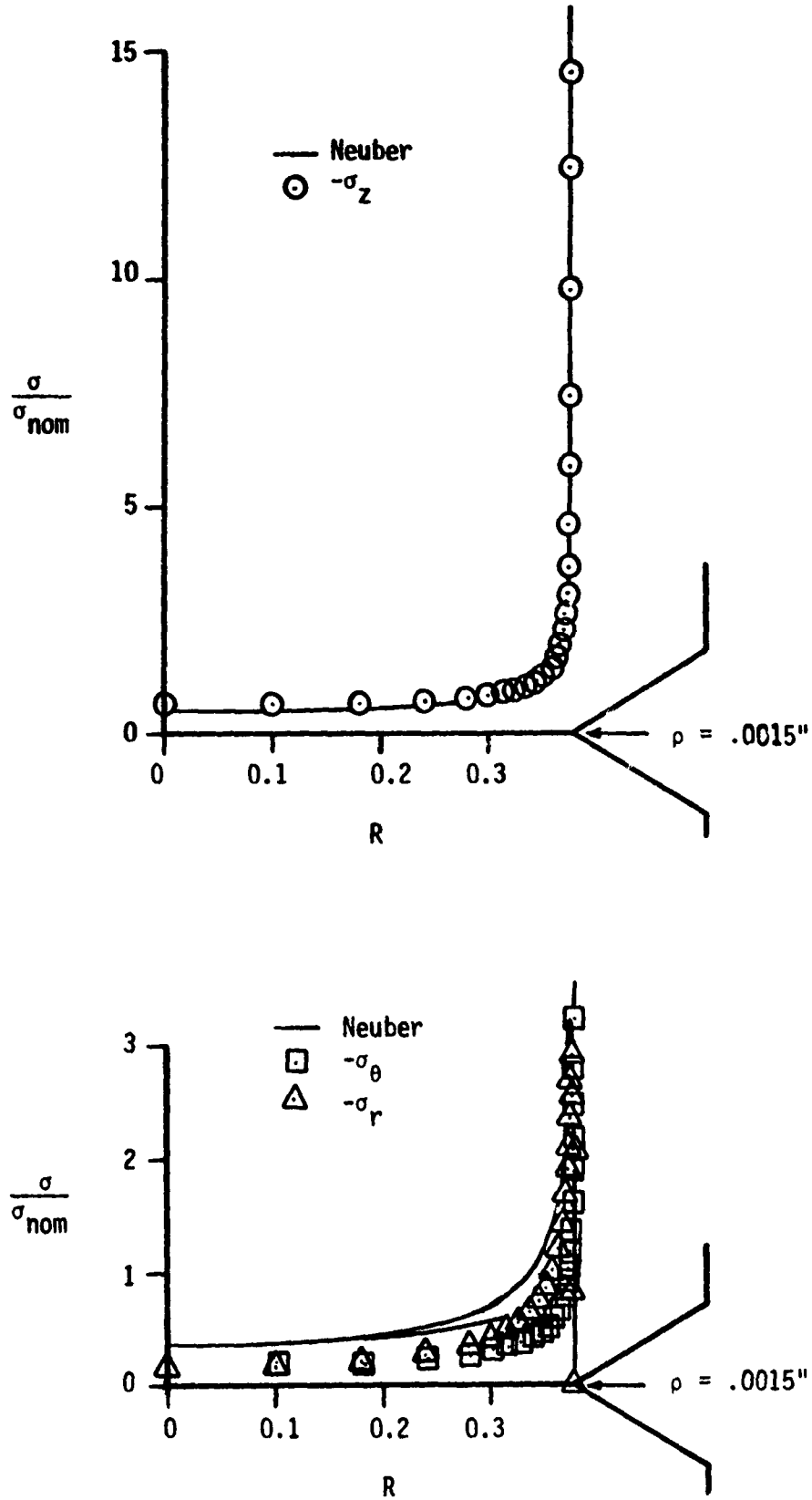

FIGURE 29. Comparison of finite-element results with Neuber solution at mid-plane for 1 in. diameter specimen with 0.0015 in. radius notch.

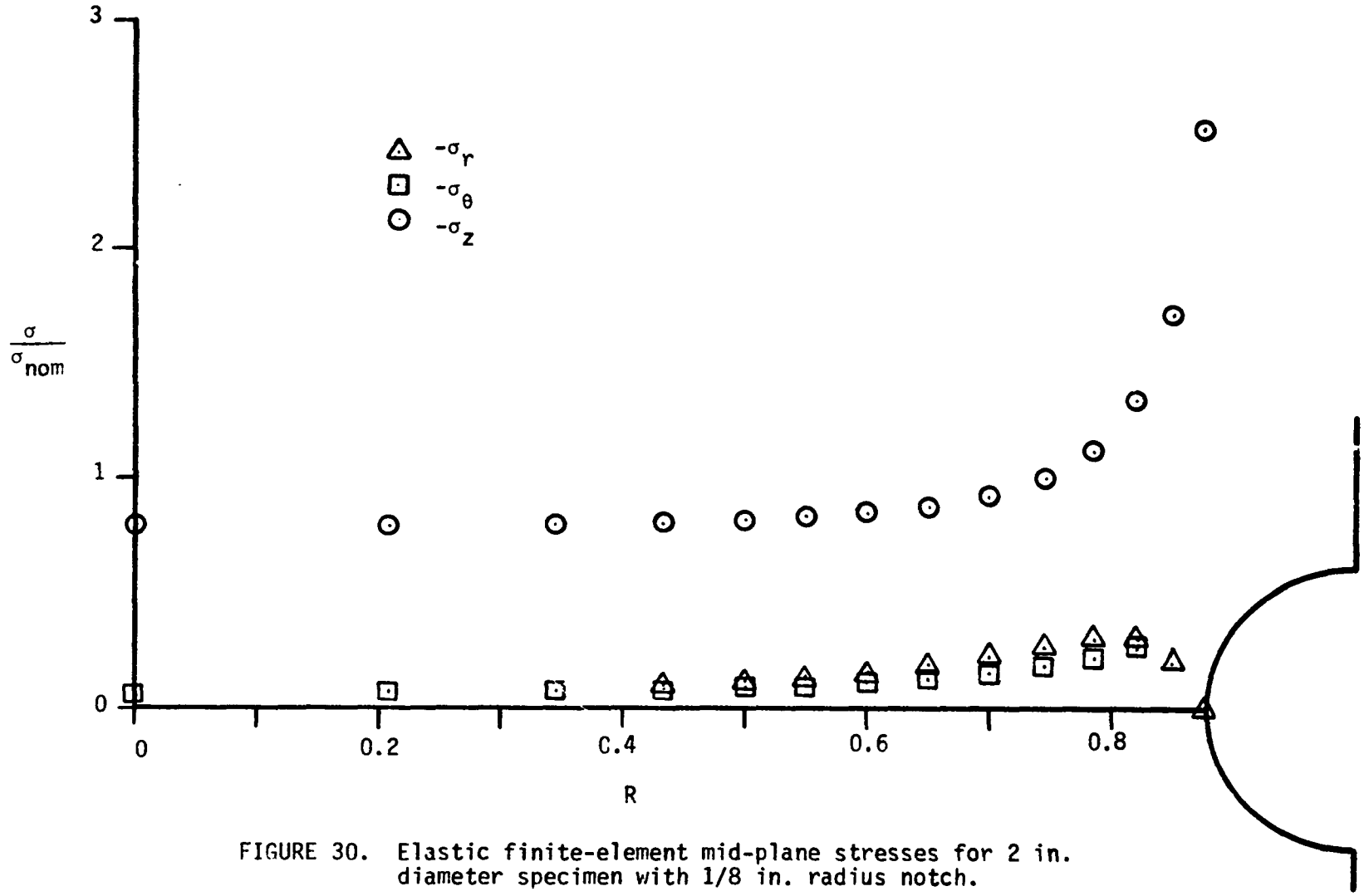

FIGURE 30. Elastic finite-element mid-plane stresses for 2 in. diameter specimen with 1/8 in. radius notch.

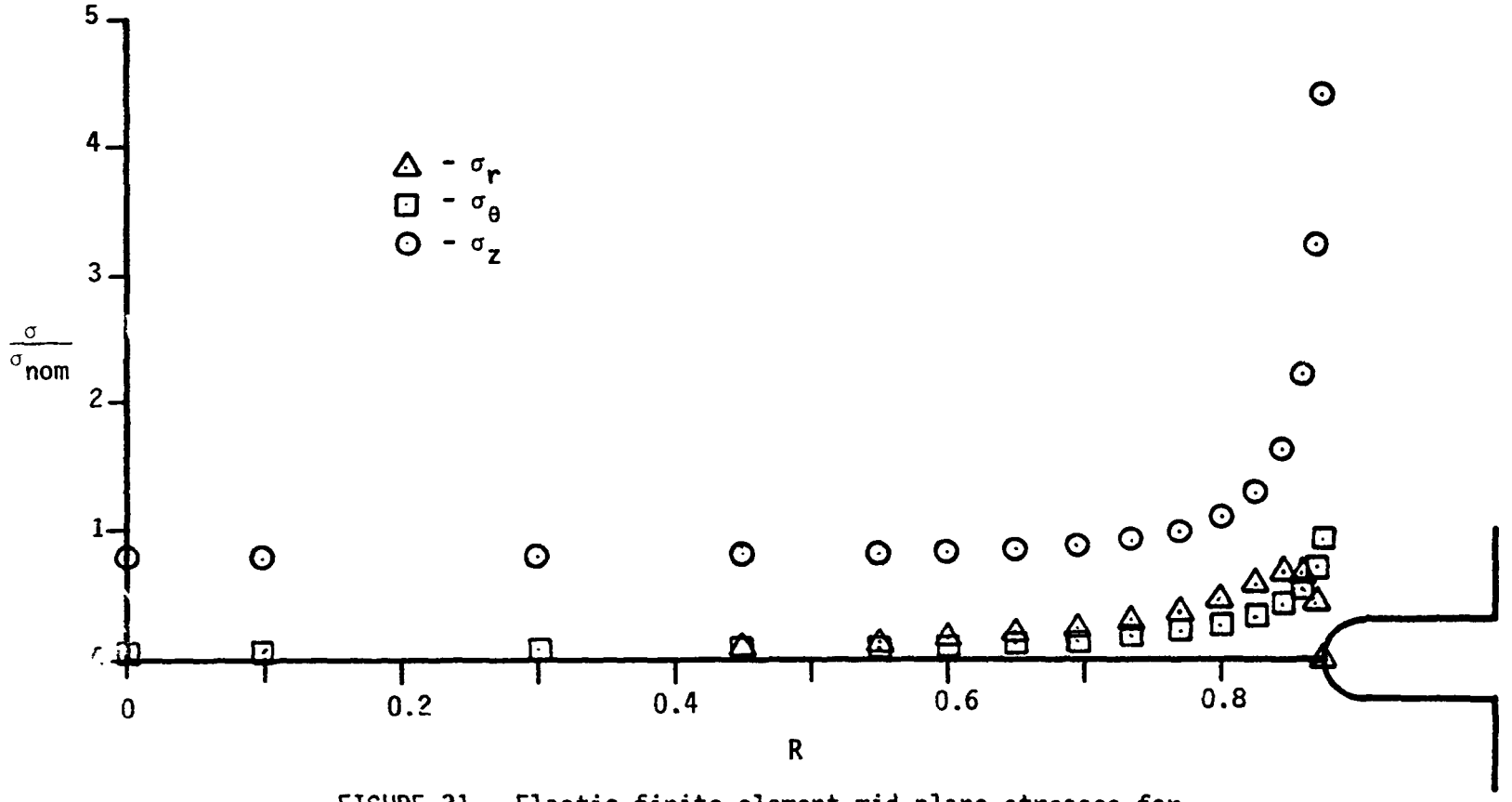

FIGURE 31. Elastic finite-element mid-plane stresses for 2 in. diameter specimen with 1/32 in. radius length.

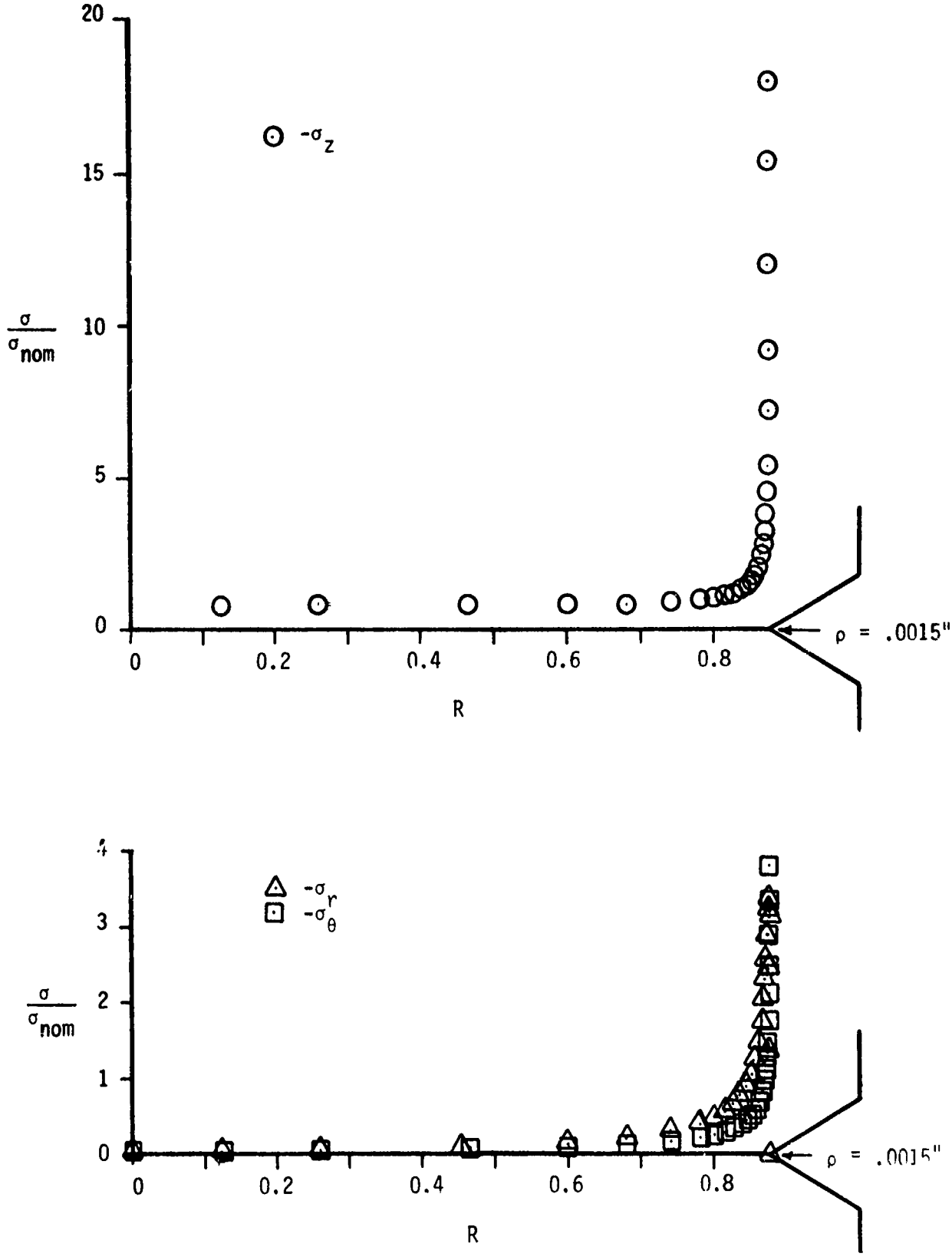

FIGURE 32. Elastic finite-element mid-plane stresses for 2 in. diameter specimen with 0.0015 in. radius notch.

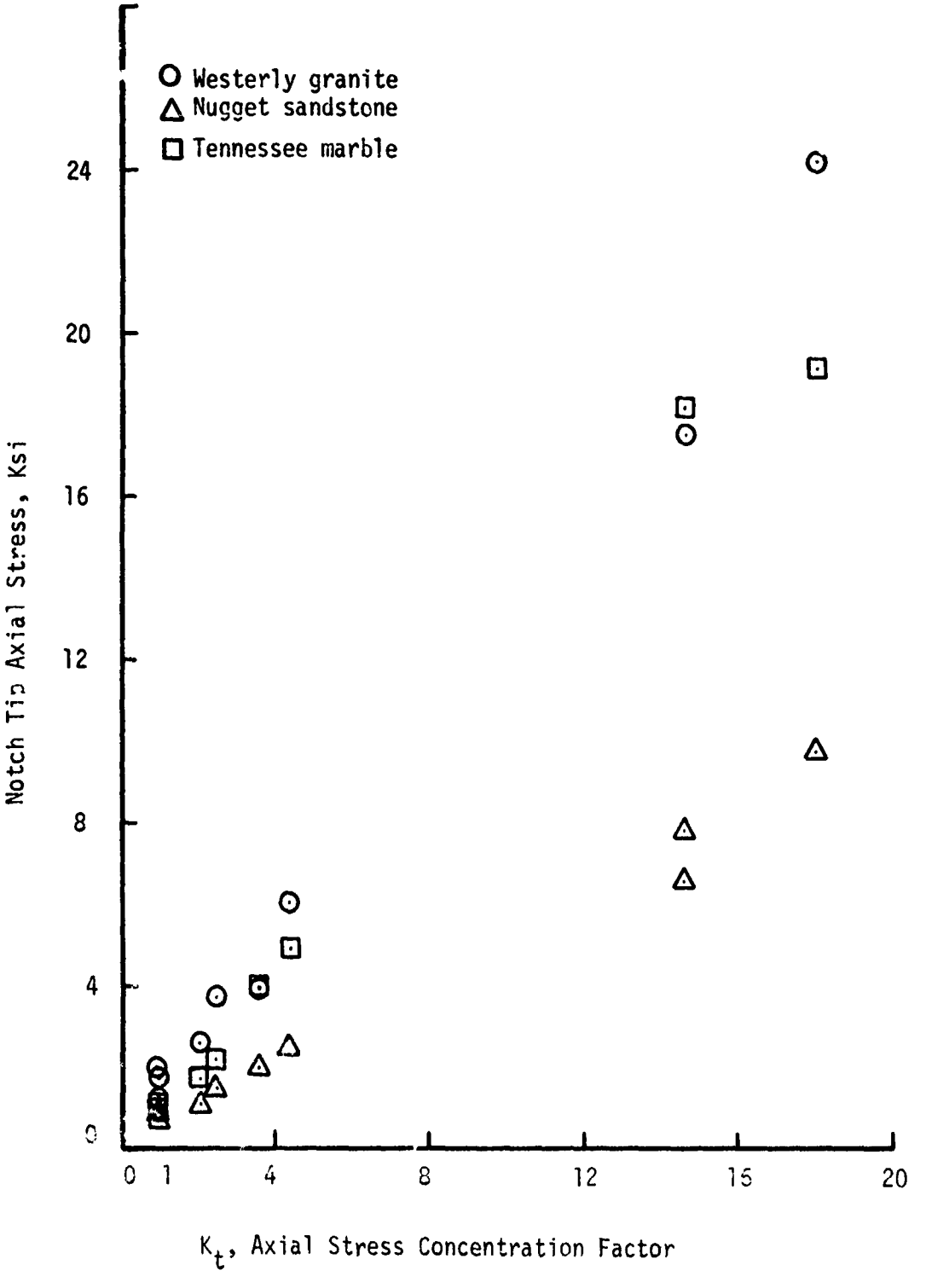

FIGURE 33. Notch tip tensi e stress in tension test specimens.

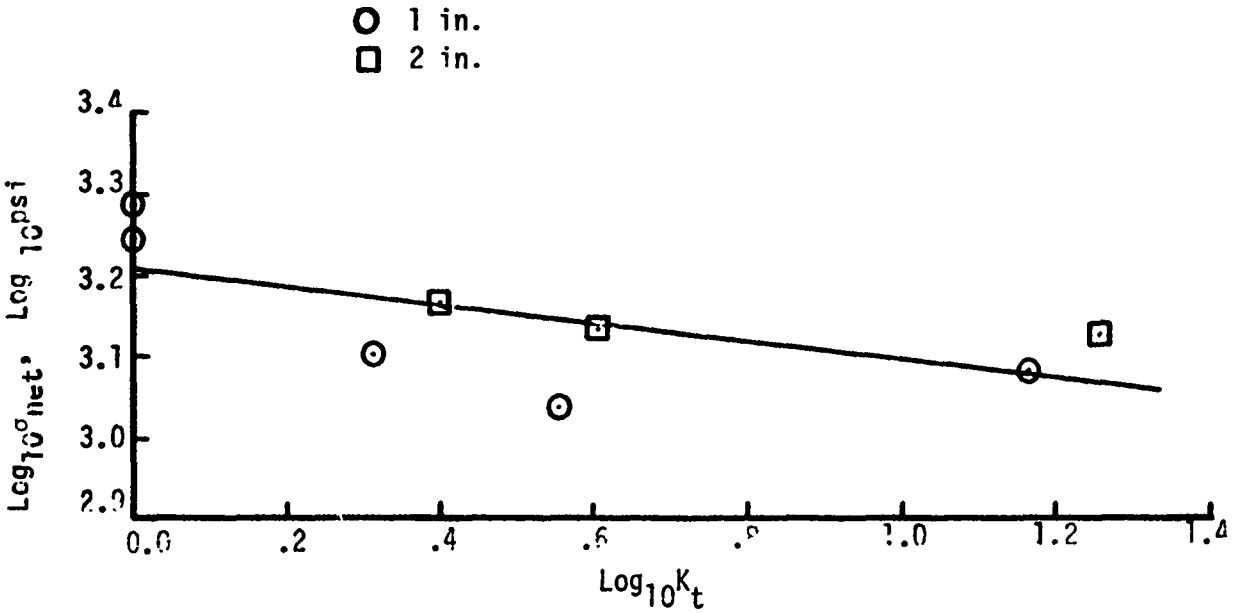

FIGURE 34. Effect of stress concentration factor on net-section stress in notched tension tests of Westerly granite.

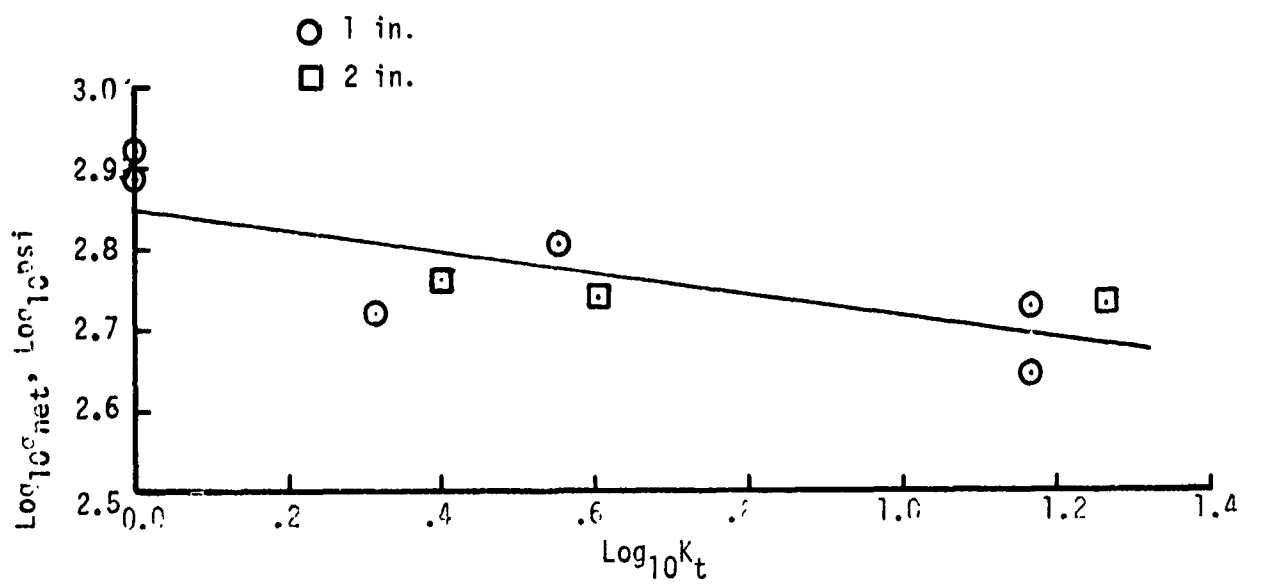

FIGURE 35. Effect of stress concentration factor on net-section stress in notched tension tests of Nugget sandstone.

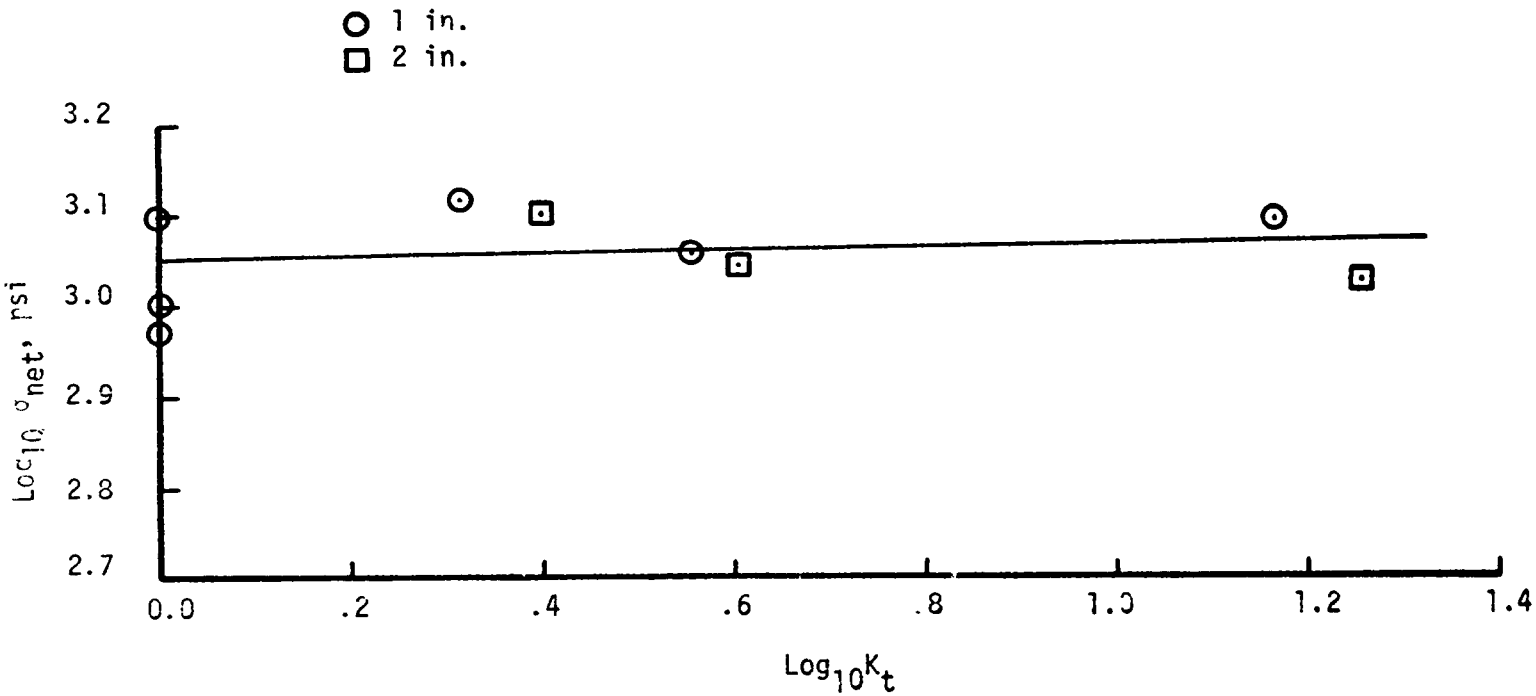

FIGURE 36. Effect of stress concentration factor on net-section stress in notched tension tests of Tennessee marble.

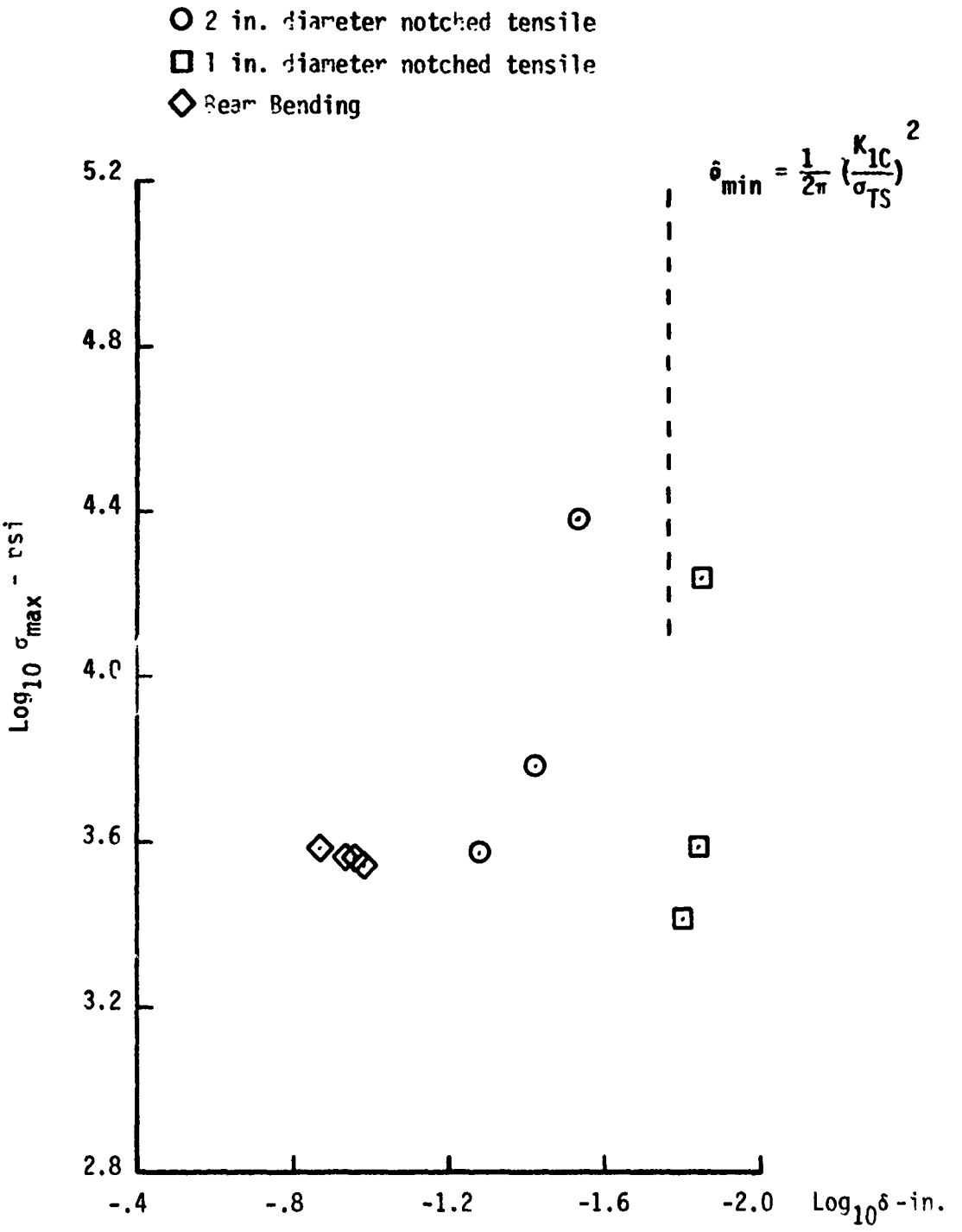

Figure 37. Critically stressed distance for non-uniform stresses in Westerly granite.

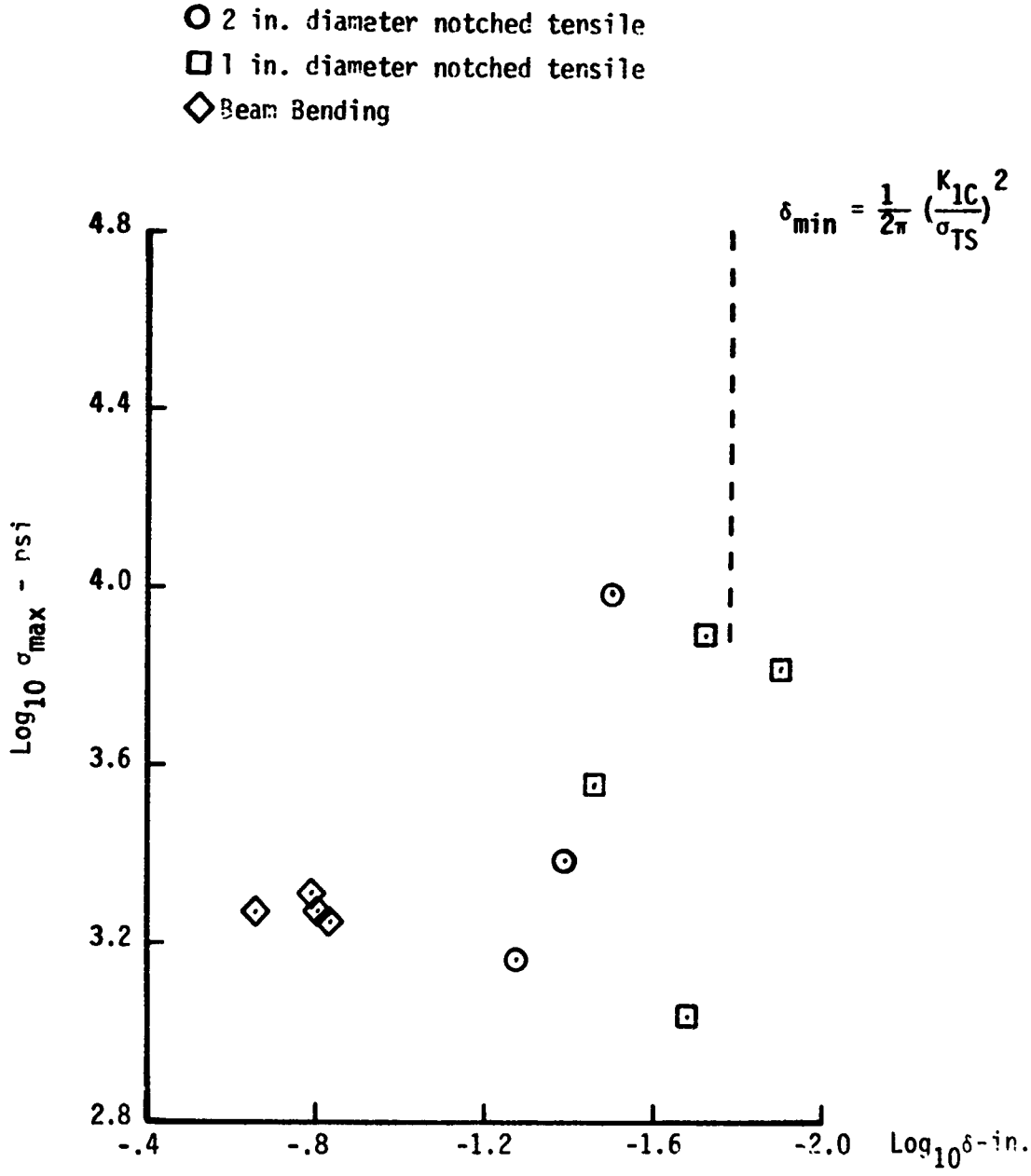

Figure 38. Critically stressed distance for non-uniform stresses in Nugget sandstone.

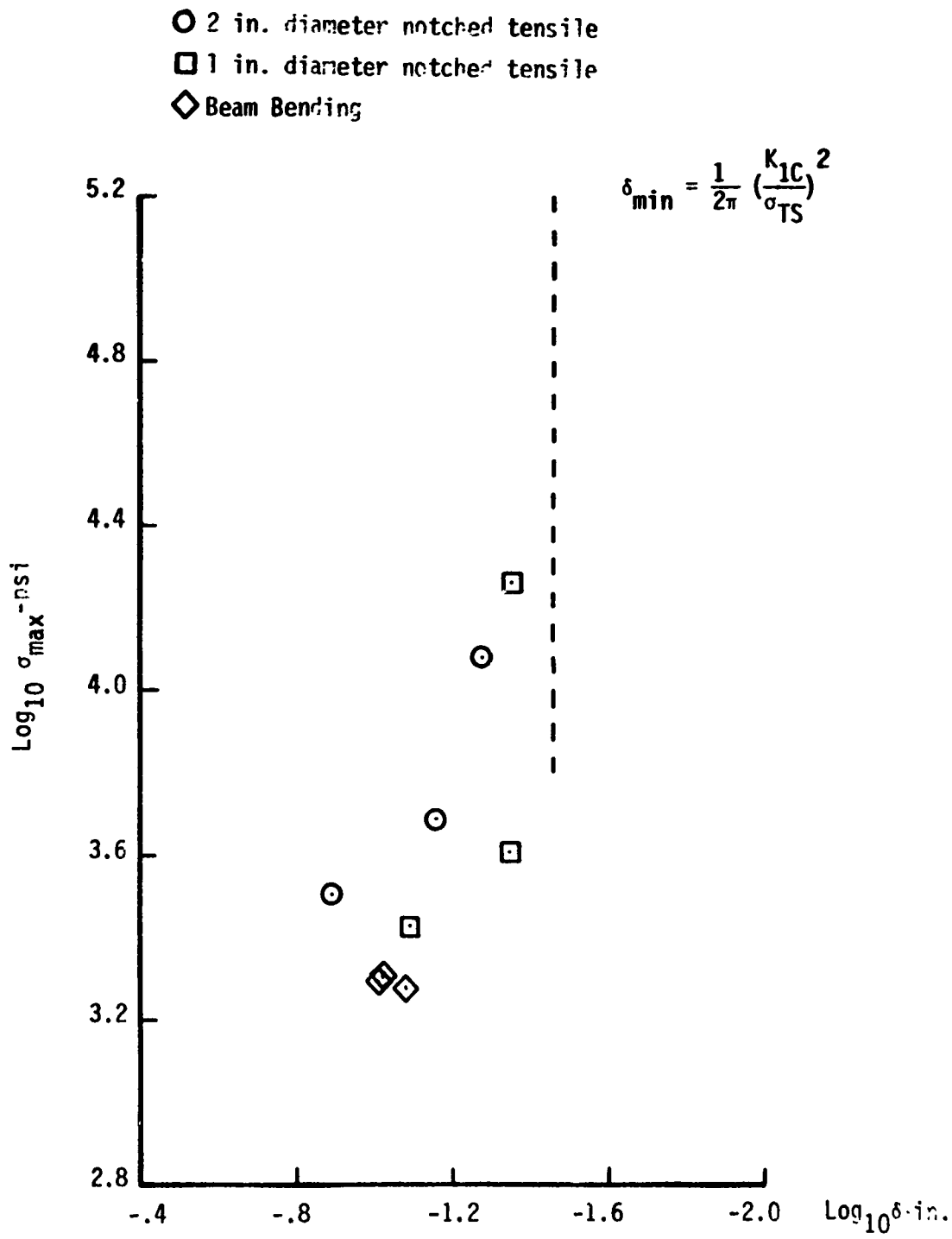

Figure 39. Critically stressed distance for non-uniform stresses in Tennessee marble.

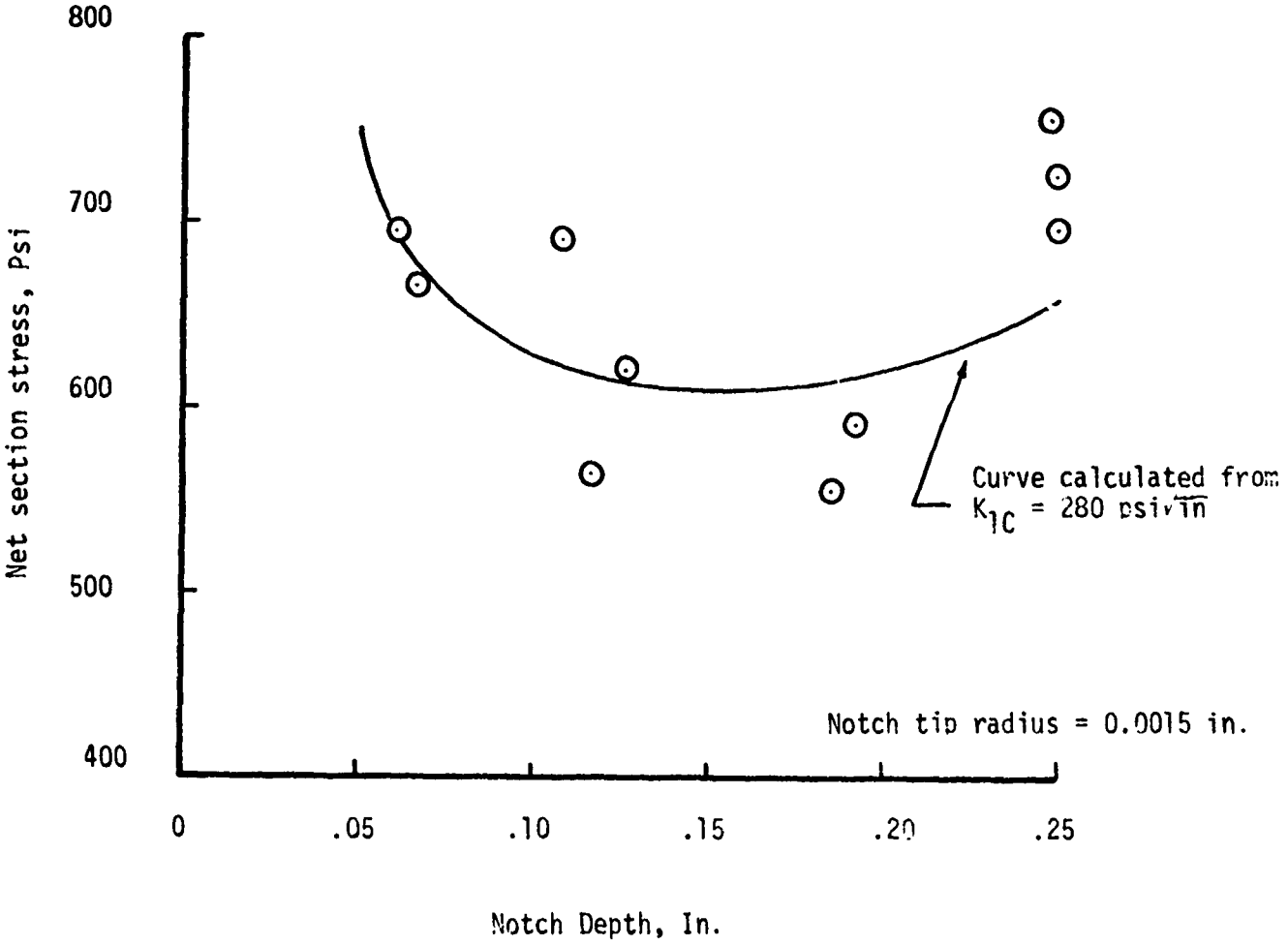

FIGURE 40. Effect of notch depth on net section stress for Nugget sandstone (Block II).

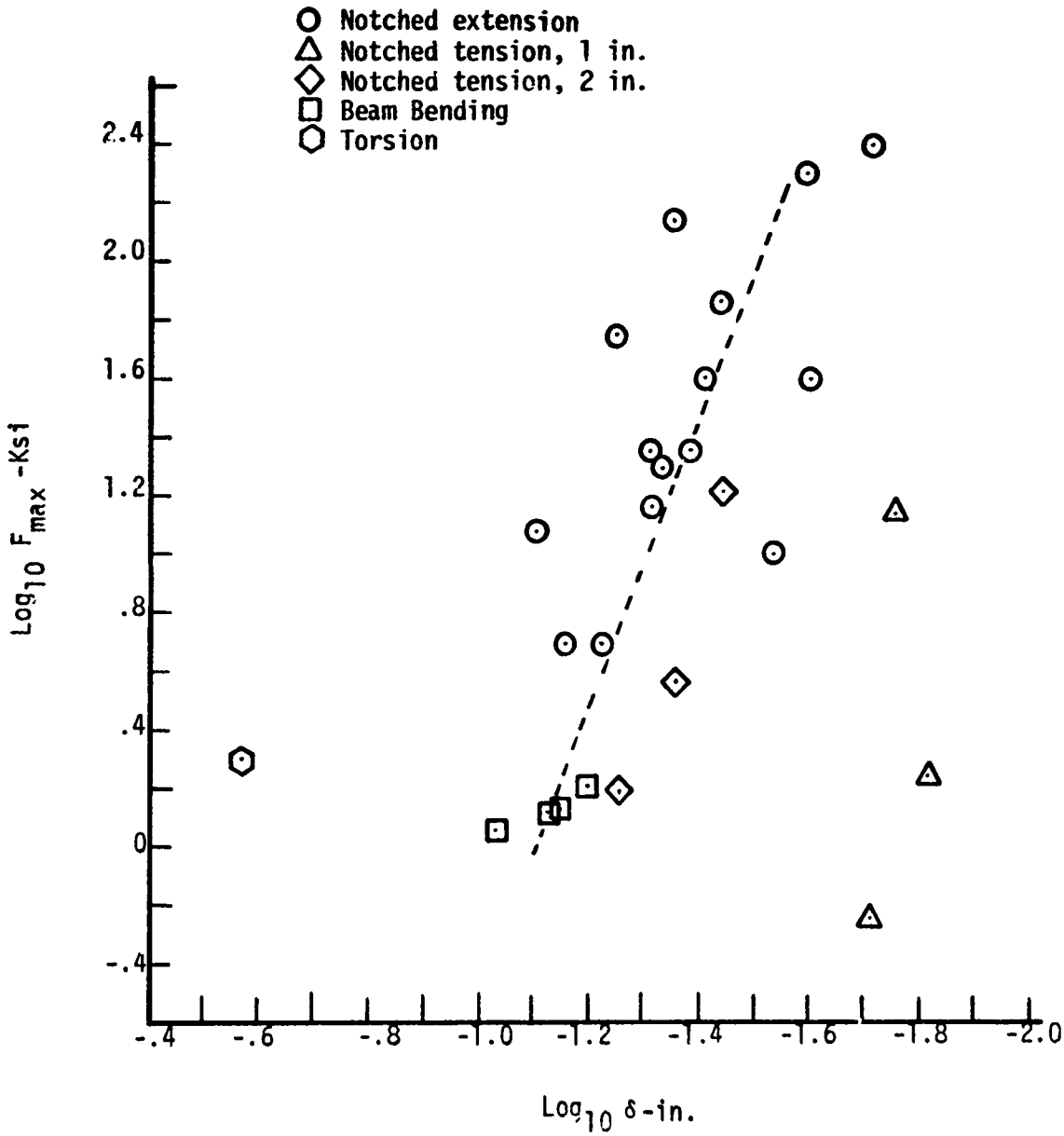

FIGURE 41. Critically stressed distance for multiaxial stress gradients in Westerly granite.

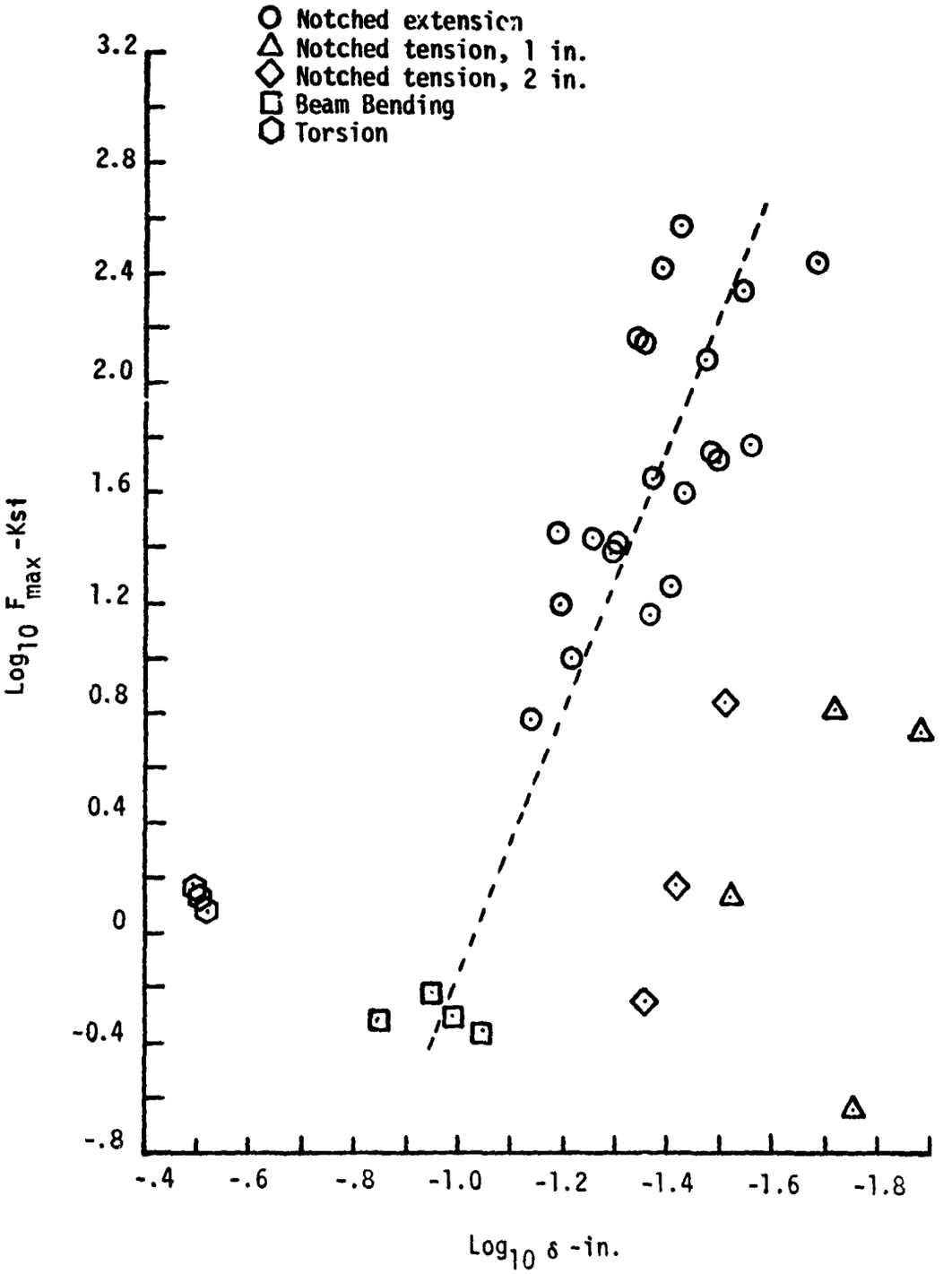

FIGURE 42. Critically stressed distance for multiaxial stress gradients in Nugget sandstone.

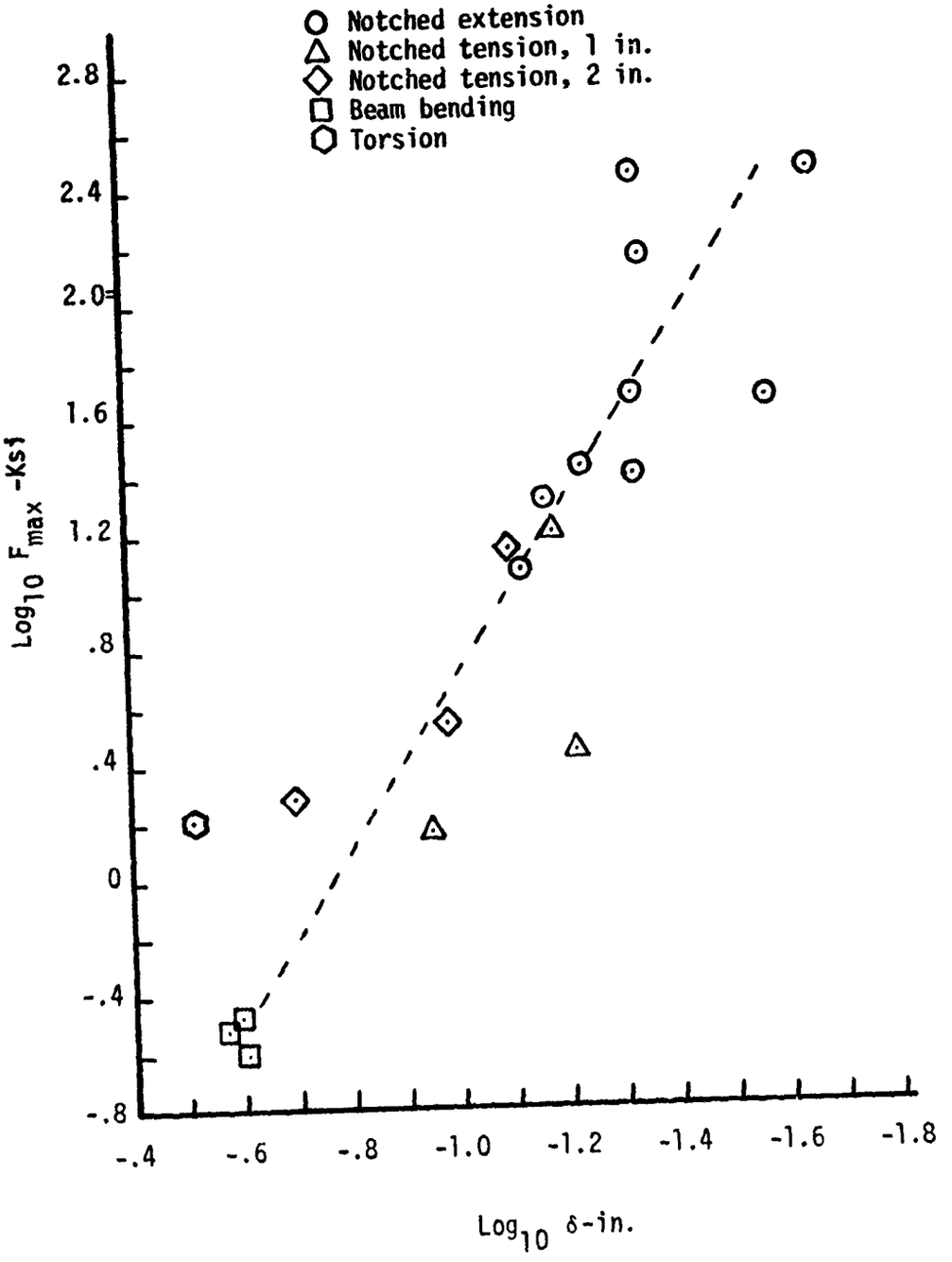

FIGURE 43. Critically stressed distance for multiaxial stress gradients in Tennessee marble.

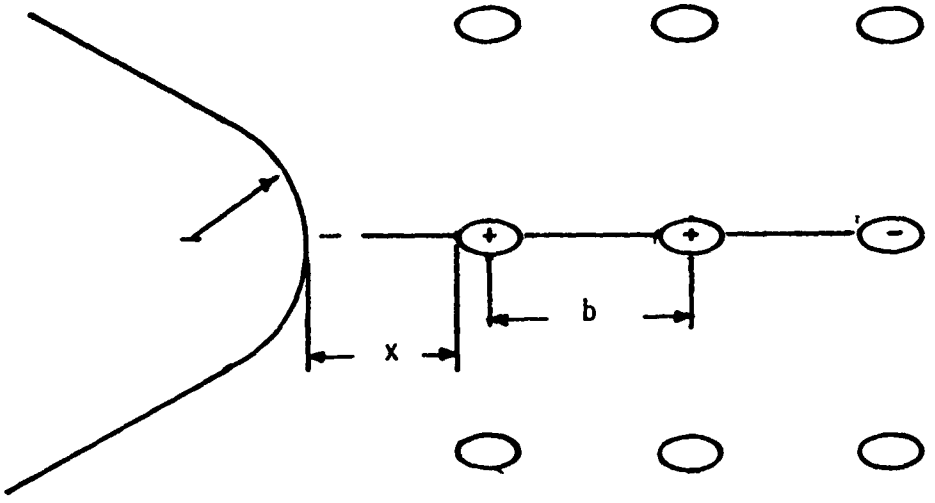

FIGURE 44. Simplified flaw model for inhomogeneous material, after Weiss, et al.

APPENDIX A

Tension Test

Specimen Number	Date of Test	Type of Rock	Notch (Inches)	Net Section Stress (psi)	Nom Diameter (Inches)	Comments
1	4-29-71	Nugget Sandstone	1/8		1	Sample broke during assembly. No data was obtained.
2	4-29-71	Westerly Granite	1/8	1256	1	
3	4-29-71	Nugget Sandstone	0.0015	82.6	1	
4	4-29-71	Westerly Granite	0.0015	1196	1	
5	4-29-71	Nugget Sandstone	Smooth	210	1	Parallel grain direction. Failure was normal to longitudinal axis.
6	4-30-71	Westerly Granite	Smooth	1260	1	
7	4-30-71	Nugget Sandstone	Smooth	518	1	
8	4-30-71	Nugget Sandstone	1/8	527	1	
9	5-4-71	Nugget Sandstone	Smooth	1069	1	Transverse grain direction.
10	5-4-71	Nugget Sandstone	Smooth	1500	1	
11	5-4-71	Nugget Sandstone	Smooth	1259	1	Parallel grain direction.
12	5-4-71	Nugget Sandstone	Smooth	455	1	Transverse grain direction.
13	5-4-71	Nugget Sandstone	Smooth	700	1	Transverse grain direction.
14	5-4-71	Nugget Sandstone	Smooth	706	1	Transverse grain direction.

Specimen Number	Date of Test	Type of Rock	Notch (Inches)	Net Section Stress (psi)	Nom Diameter (Inches)	Comments
87		Tennessee Marble	1/8		1	Epoxy broke on end tab.
89	8-2-71	Tennessee Marble	Smooth	885	3/4	Epoxy broke on end tab on first test. Second test was run and was good.
88	8-3-71	Nugget Sandstone	1/32	635	1	
90	8-6-71	Tennessee Marble	Smooth	735	3/4	
91	8-6-71	Tennessee Marble	Smooth	928	3/4	
95	8-6-71	Tennessee Marble	1/32	1140	1	
96	8-6-71	Tennessee Marble	0.0015	1240	1	
99	8-13-71	Westerly Granite	1/32	1090	1	
100	8-13-71	Tennessee Marble	1/8	1310	1	
101	8-13-71	Westerly Granite	Smooth	1190	3/4	
102	8-1 -71	Nugget Sandstone	Smooth	830	3/4	
110	8-19-71	Nugget Sandstone	0.0015	535	1	
111	8-19-71	Nugget Sandstone	0.0015	442	1	

Specimen Number	Date of Test	Type of Rock	Notch (Inches)	Net Section Stress (psi)	Nom Diameter (Inches)	Comments
115	2-5-72	Westerly Granite	Smooth	1935	1	
116	2-14-72	Westerly Granite	Smooth	1745	1	
117	2-14-72	Nugget Sandstone	Smooth	733	1	
118	2-14-72	Tennessee Marble	Smooth	1013	1	

Specimen Number	Date of Test	Type of Rock	Notch (Inches)	Net Section Stress (psi)	Nom Diameter (Inches)	Comments
5-2	12-15-71	Nugget Sandstone	0.0015-2	538	2	
6-2	12-15-71	Nugget Sandstone	1/8-2	576	2	
9-2	12-15-71	Tennessee Marble	1/8-2	1260	2	
3-2	12-20-71	Westerly Granite	1/8-2	1470	2	
4-2	12-20-71	Nugget Sandstone	1/32-2	553	2	Epoxy on end tab broke on first test. Second test ran and was good.
7-2	12-20-71	Tennessee Marble	1/32-2	1110	2	
8-2	12-20-71	Tennessee Marble	0.0015-2	1060	2	
1-2	12-22-71	Westerly Granite	1/32-2	1370	2	
2-2	12-22-71	Westerly Granite	0.0015-2	1340	2	
11-2	12-22-71	Nugget Sandstone	Smooth-2	732	2	
12-2	12-22-71	Tennessee Marble	Smooth-2	1260	2	
10-2	12-30-71	Westerly Granite	Smooth-2	1920	2	Epoxy on end tabs broke. Value given is for that test.
13-2	2-2-72	Westerly Granite	Smooth-2	1390	2	Two tests run, end tabs broke on both tests. Value is maximum value reached

APPENDIX B

Bending Tests

Specimen Number	Rock Type	Length of Case (Inches)	Height of Specimen (in)	Maximum Load (lbs)	Bending Moment (in-lb)	Bending Stresses (psi)
B-1	Tennessee Marble	1.003	0.497	104	78.04	1890
B-2	Tennessee Marble	1.010	0.538	128	96.0	1970
B-3	Tennessee Marble	1.005	0.510	117	87.7	2014
B-4	Westerly Granite	1.050	0.564	286	214.5	3853
B-5	Westerly Granite	1.058	0.508	222	166.5	3659
B-6	Westerly Granite	1.047	0.493	197	147.7	3484
B-7	Westerly Granite	1.050	0.497	210	157.5	3644
B-8	Nugget Sandstone	1.025	0.535	121	91.8	1877
B-9	Nugget Sandstone	1.018	0.520	108	81.4	1775
B-10	Nugget Sandstone	1.027	0.522	127	95.1	2040
B-11	Nugget Sandstone	1.026	0.753	240	180.	1856

APPENDIX C

Torsion Tests

Specimen Number	Date of Test	Type of Rock	Outside Diameter (in)	Notch Diameter (in)	Notch Type	Failure(in-Torque lbs)	Nom. Shear Stress (psi)	Comments
1	3-7-71	Nugget Sandstone		None	None	400	2140	No end tabs were used, test apparatus was griped to rock. Break was good.
2	3-7-71	Nugget Sandstone		None	None	400	2140	No end tabs were used, test apparatus was griped to rock. Break was good.
3	3-12-71	Nugget Sandstone		None	None	300	1600	Eastman 910 was used to hold end tabs on. Glue failure instead.
4	3-12- 1	Nugget Sandstone		None	None	300	1600	Eastman 910 used to hold end tabs on. Glue failed instead of rock.
5	3-18-71	Nugget Sandstone		None	None	440	2350	Liquid steel used to hold end tabs on. Held well.
6	3-18-71	Nugget Sandstone		None	None	510	2720	Liquid steel used to hold end tabs on. Held well.
7	4-5-71	Nugget Sandstone		None	None	407.5	2180	First test ran with torque cell to determine failure torque.
8	4-5-71	Nugget Sandstone		None	None	416	2220	
9	4-30-71	Nugget Sandstone	1000"	None	None	442	2360	
10	4-30-71	Nugget Sandstone	1001"	0.775	0.0015	120	1442	Ends were out of line at the end of test, possible rock put in on angle.
11	4-30-71	Nugget Sandstone	0.999"	0.746	1/8	234	2820	
12	4-30-71	Westerly Granite	1.000"	None	None	736	3930	
13	4-30-71	Westerly Granite	1,002"	0.775	0.0015	500	6030	

Specimen Number	Date or Test	Type of Rock	Outside Diameter (in)	Notch Diameter (in)	Notch Type	Failure (in Torque -lb)	Nom. Shear Stress (psi)	Comments
14	4-30-71	Westerly Granite	0.999	0.745	1/8	454	5470	
15	4-30-71	Westerly Granite	1.001		1/8	625		Notch put in rock longitudinally.
16	4-30-71	Nugget Sandstone	0.999		1/8	478		Notch put in rock longitudinally.
23	5-21-71	Nugget Sandstone	0.998		1/32	425	5120	
47	5-21-71	Westerly Granite	1.00		1/32	582	7030	
70	6-15-71	Tennessee Marble	0.999		None	527	2810	
71	6-15-71	Tennessee Marble	0.999	0.798	1/8	491	5920	
72	6-15-71	Tennessee Marble	0.998		0.0015	529	6370	
73	6-15-71	Tennessee Marble	0.999		1/32	482	5700	
107	8-10-71	Nugget Sandstone	0.999		None			
108		Nugget Sandstone	0.999		0.0015			

APPENDIX D

Extension

Specimen Number	Date of Test	Type of Rock	Specimen Diameter (inches)	Notch Type	Confining Pressure (ksi)	Failure Stress (psi)	Comments
1	4-5-71	Nuggett Sandstone	0.750	None	None		Error in test procedure caused specimen to fail in compression
2	4-6-71	Nugget Sandstone	0.717	None	15.39		Epoxy on and tabs failed.
3	5-19-71	Nugget Sandstone	0.734	None	30.4	2300	Failed tygon tubing making exact failure load uncertain.
4	5-19-71	Nugget Sandstone	0.730	None	30.0	7700	Error in testing, exact failure stress unknown.
5	6-8-71	Westerly Granite	0.743	None	4.93		Epoxy on end tabs failed.
6	6-8-71	Nugget Sandstone	0.718	None	4.9		Epoxy on end tabs failed.
7	6-10-71	Nugget Sandstone	0.999	1/8	20.0	1500	
8	6-9-71	Westerly Granite	1.001	1/8	5	1120	
9	6-9-71	Nugget Sandstone	0.999	0.0015	5	260	
10	6-10-71	Westerly Granite	0.999	0.0015	20.0	2120	
11	6-15-71	Nugget Sandstone	0.750	None	15	900	
12	6-15-71	Nugget Sandsonte	0.750	None	10	710	Possibly early failure of epoxy on end tabs.
13	6-22-71	Nugget Sandstone	1.000	1/8	5	1200	

Specimen Number	Date of Test	Type of Rock	Specimen Diameter (inches)	Notch Type	Confining Pressure (ksi)	Failure Stress (psi)	Comments
14	6-22-71	Nugget Sandstone	0.999	1/8	10	900	
15	6-22-71	Westerly Granite	1.001	0.0015	5	1100	
16	6-22-71	Westerly Granite	1.002	1/8	5	2000	
17		Westerly Granite	1.000	1/32			
18	7-9-71	Westerly Granite	1.001	1/32	10	13200	
19	6-25-71	Westerly Granite	1.000	1/32	none		Problem with equipment during the run.
20		Westerly Granite	0.998	1/32			Failure of epoxy on end tabs.
21		Westerly Granite	0.998	1/32	22.18	1920	Specimen may have saturated before it broke.
22	6-23-71	Nugget Sandstone	1.001	1/32	10	990	Specimen may have saturated before it broke.
24	6-23-71	Nugget Sandstone	1.000	1/32	20	1000	Specimen may have saturated before it broke.
25	6-23-71	Nugget Sandstone	1.000	1/32	30	4700	Specimen may have saturated before it broke.
26		Nugget Sandstone	0.999	1/32			
27	6-22-71	Nugget Sandstone	1.000	1/32	5	1090	

Specimen Number	Date of Test	Type of Rock	Specimen Diameter (inches)	Notch Type	Confining Pressure (ksi)	Failure Stress (psi)	Comments
28	7-9-71	Westerly Granite	1.000	1/32	5	6020	
29	7-8-71	Westerly Granite	1.000	0.0015	10	10200	
30	6-24-71	Westerly Granite	0.999	0.0015	30		The load cell shorted out during the test and the sample was saturated.
31	7 9-71	Westerly Granite	1.000	1/32	20	12600	
32	6-23-71	Nugget Sandstone	0.998	0.0015	10	1200	Sample may have been saturated.
33	6-23-71	Nugget Sandstone	0.999	0.0015	30	2600	Sample may have been saturated.
34	6-23-71	Nugget Sandstone	1.001	0.0015	30	7800	Sample may have been saturated.
35	6-30-71	Nugget Sardstone	1.000	0.0015	10	920	
36	6-30-71	Nugget Sandstone	0.996	0.0015	20	100	
37	6-29-71	Nugget Sandstone	0.998	0.0015	30	700	The piston broke during the test.
38	7-15-71	Westerly Granite	1.000	1/8	10	2610	
39	7-16-71	Westerly Granite	1.000	1/8	30	800	
40	6-25-71	Westerly Granite	0.998	1/8	15		Trouble with the load cell readings.

Specimen Number	Date of Test	Type of Rock	Specimen Diameter (inches)	Notch Type	Confining Pressure (ksi)	Failure Stress (psi)	Comments
41	6-24-71	Westerly Granite	1.000	1/8	20	1100	
42		Nugget Sandstone	0.993	1/8			
43	7-12-71	Nugget Sandstone	0.999	1/8	30	3000	
44	6-23-71	Nugget Sandstone	0.997	1/8	30	3800	Sample may have been saturated.
45	7-16-71	Nugget Sandstone	1.00	1/8	30	300	Sample may have been saturated.
46		Westerly Granite	0.995	1/8			
48	7-15-71	Westerly Granite	0.999	0.0015	10	6700	
49	6-21-71	Nugget Sandstone	0.750	None	5		Specimen saturated.
50	6-21-71	Nugget Sandstone	0.750	None	5	860	
51	6-22-71	Westerly Granite	0.750	None	10	800	
52	6-22-71	Westerly Granite	0.750	None	5	840	
53	7-12-71	Westerly Granite	0.993	1/8	30	3200	
54	7-12-71	Westerly Granite	1.000	0.0015	10	3700	

Specimen Number	Date of Test	Type of Rock	Specimen Diameter (inches)	Notch Type	Confining Pressure (ksi)	Failure Stress (psi)	Comments
55	7-7-71	Nugget Sandstone	0.999	1/32	10	11300	
56		Nugget Sandstone	0.999	1/32			
57		Nugget Sandstone	0.994	1/32			
58	8-5-71	Tennessee Marble	0.999	1/8	30		
59	8-3-71	Tennessee Marble	0.999	1/8	20	1620	
60	7-28-71	Tennessee Marble	0.99[illegible]	1/8		1780	
61		Tennessee Marble	0.999	1/8			
62	8-5-71	Tennessee Marble	0.998	1/32	30	7400	
63	8-5-71	Tennessee Marble	0.994	1/32	20	250	
64	7-28-72	Tennessee Marble	1.001	1/32	10	600	
65		Tennessee Marble	0.999	1/32			
66	8-5-71	Tennessee Marble	0.999	0.0015	30	7400	
67	8-5-71	Tennessee Marble	0.998	0.0015	20	10760	

Specimen Number	Date of Test	Type of Rock	Specimen Diameter (inches)	Notch Type	Confining Pressure (ksi)	Failure Stress (psi)	Comments
68	7-28-71	Tennessee Marble	1.000	0.0015	10	1100	
69		Tennessee Marble	0.999	0.0015			
74	7-15-71	Nugget Sandstone	1.000	1/8	20		
75	7-15-71	Nugget Sandstone	0.997	0.0015	10	200	
76	7-16-71	Westerly Granite	1.001	0.0015	30	7400	
77	8-4-71	Westerly Granite	0.970	1/32	20	1480	
78	8-5-71	Westerly Granite	0.936	1/32	30	8300	
79		Westerly Granite	0.946	1/32			
80	8-4-71	Nugget Sandstone	0.993	1/32	20	600	
81	8-4-71	Nugget Sandstone	0.997	1/32	30	4050	
82		Nugget Sandstone	0.996	1/32			
83		Nugget Sandstone	0.999	1/32			
84	7-29-71	Westerly Granite	0.745	None	10	1780	Specimen may have been saturated.

Specimen Number	Date of Test	Type of Rock	Specimen Diameter (inches)	Notch Type	Confining Pressure (ksi)	Failure Stress (psi)	Comments
85	7-30-71	Westerly Granite	0.740	None	20	3000	Specimen saturated when removed. Failed during trouble with controls, broke at both ends
86	7-30-71	Westerly Granite		None	30	800	Specimen may have been saturated.
92		Nugget Sandstone	0.750	None			
93		Westerly Granite	0.747	None			
94	8-4-71	Nugget Sandstone	0.737	None	30	1800	
97	8-6-71	Nugget Sandstone		None	20	2930	Broke at both ends.
98	8-6-71	Nugget Sandstone		None	10	2300	
103		Tennessee Marble	0.746	None			Broke before test.
104	8-12-71	Tennessee Marble	0.999	0.0015	20	21450	
105	8-12-71	Tennessee Marble	0.737	None	30	31800	
106	8-12-71	Tennessee Marble	0.751	None	20	23300	
109	8-17-71	Tennessee Marble	0.738	None	10	11740	
112	8-20-71	Tennessee Marble	0.750	None	5	6610	

Specimen Number	Date of Test	Type of Rock	Specimen Diameter (inches)	Notch Type	Confining Pressure (ksi)	Failure Stress (psi)	Comments
113	8-20-71	Westerly Granite	0.747	None	5	7760	
114	8-20-71	Nugget Sandstone	0.747	None	5	7590	